Isotopic constraints on glacial/interglacial changes in the oceanic nitrogen budget

Curtis Deutsch,[1,2] Daniel M. Sigman,[3] Robert C. Thunell,[4] Anna Nele Meckler,[5] and Gerald H. Haug[6]

Received 18 November 2003; revised 17 May 2004; accepted 16 July 2004; published 28 October 2004.

[1] We investigate the response of the $^{15}N/^{14}N$ of oceanic nitrate to glacial/interglacial changes in the N budget, using a geochemical box model of the oceanic N cycle that includes N_2 fixation and denitrification in the sediments and suboxic water column. This model allows us to quantify the isotopic response of different oceanic nitrate pools to deglacial increases in water column and sedimentary denitrification, given a range of possible feedbacks between nitrate concentration and N_2 fixation/denitrification. This response is compared to the available paleoceanographic data, which suggest an early deglacial maximum in nitrate $^{15}N/^{14}N$ in suboxic zones and no significant glacial-to-late Holocene change in global ocean nitrate $^{15}N/^{14}N$. Consistent with the work of *Brandes and Devol* [2002], we find that the steady state $^{15}N/^{14}N$ of oceanic nitrate is controlled primarily by the fraction of total denitrification that occurs in the water column. Therefore a deglacial peak in the ratio of water column-to-sediment denitrification, caused by either a strong feedback between water column denitrification and the N reservoir or by an increase in sediment denitrification due to sea level rise, can explain the observed deglacial $^{15}N/^{14}N$ maximum in sediments underlying water column denitrification zones. The total denitrification rate and the mean ocean nitrate concentration are also important determinants of steady state nitrate $^{15}N/^{14}N$. For this reason, modeling a realistic deglacial $^{15}N/^{14}N$ maximum further requires that the combined negative feedbacks from N_2 fixation and denitrification are relatively strong, and N losses are relatively small. Our results suggest that the glacial oceanic N inventory was at most 30% greater than today's and probably less than 10% greater. *INDEX TERMS:* 4267 Oceanography: General: Paleoceanography; 4805 Oceanography: Biological and Chemical: Biogeochemical cycles (1615); 4845 Oceanography: Biological and Chemical: Nutrients and nutrient cycling; 4870 Oceanography: Biological and Chemical: Stable isotopes; *KEYWORDS:* feedback, nitrogen isotopes, paleoceanography

Citation: Deutsch, C., D. M. Sigman, R. C. Thunell, A. N. Meckler, and G. H. Haug (2004), Isotopic constraints on glacial/interglacial changes in the oceanic nitrogen budget, *Global Biogeochem. Cycles*, *18*, GB4012, doi:10.1029/2003GB002189.

1. Introduction

[2] The nitrogen cycle plays a central role in the biogeochemistry of the ocean. As an essential nutrient, biologically available (or "fixed") N has the potential to limit biological productivity over large regions of the ocean. Changes in the N cycle are of growing interest in research at the interface between climate and biogeochemistry. Several lines of evidence now point to important influences of climate change on the N budget [*Altabet et al.*, 1995; *Ganeshram et al.*, 1995; *Karl et al.*, 1997], and hypotheses have been put forward for indirect influences of the marine N budget on climate [*Altabet et al.*, 2002; *Falkowski*, 1997; *Ganeshram et al.*, 2000; *McElroy*, 1983; *Suthhof et al.*, 2001]. A change in the oceanic inventory of fixed N (which is dominated by nitrate, NO_3^-) would be expected to impact the biological carbon pump in the low-latitude ocean, where the major nutrients (nitrate and phosphate) limit productivity. As a result, an increase in the N inventory during the last ice age has been offered as a possible cause for lower glacial atmospheric pCO_2 [*McElroy*, 1983].

[3] The magnitude of sources and sinks of fixed N in the modern ocean are probably not known to better than a factor of 2. Nevertheless, it is now believed that the residence time of oceanic N is roughly 2–3 kyr [*Brandes and Devol*, 2002; *Gruber and Sarmiento*, 1997], which is short in the context of glacial/interglacial climate change, such that conceivable imbalances could cause large changes in the

[1]Program in Atmospheric and Oceanic Sciences, Princeton University, Princeton, New Jersey, USA.
[2]Now at Program on Climate Change, University of Washington, Seattle, Washington, USA.
[3]Department of Geosciences, Princeton University, Princeton, New Jersey, USA.
[4]Department of Geological Sciences, University of South Carolina, Columbia, South Carolina, USA.
[5]Geological Institute, Zurich, Switzerland.
[6]Geoforschungszentrum Potsdam, Potsdam, Germany.

0886-6236/04/2003GB002189$12.00

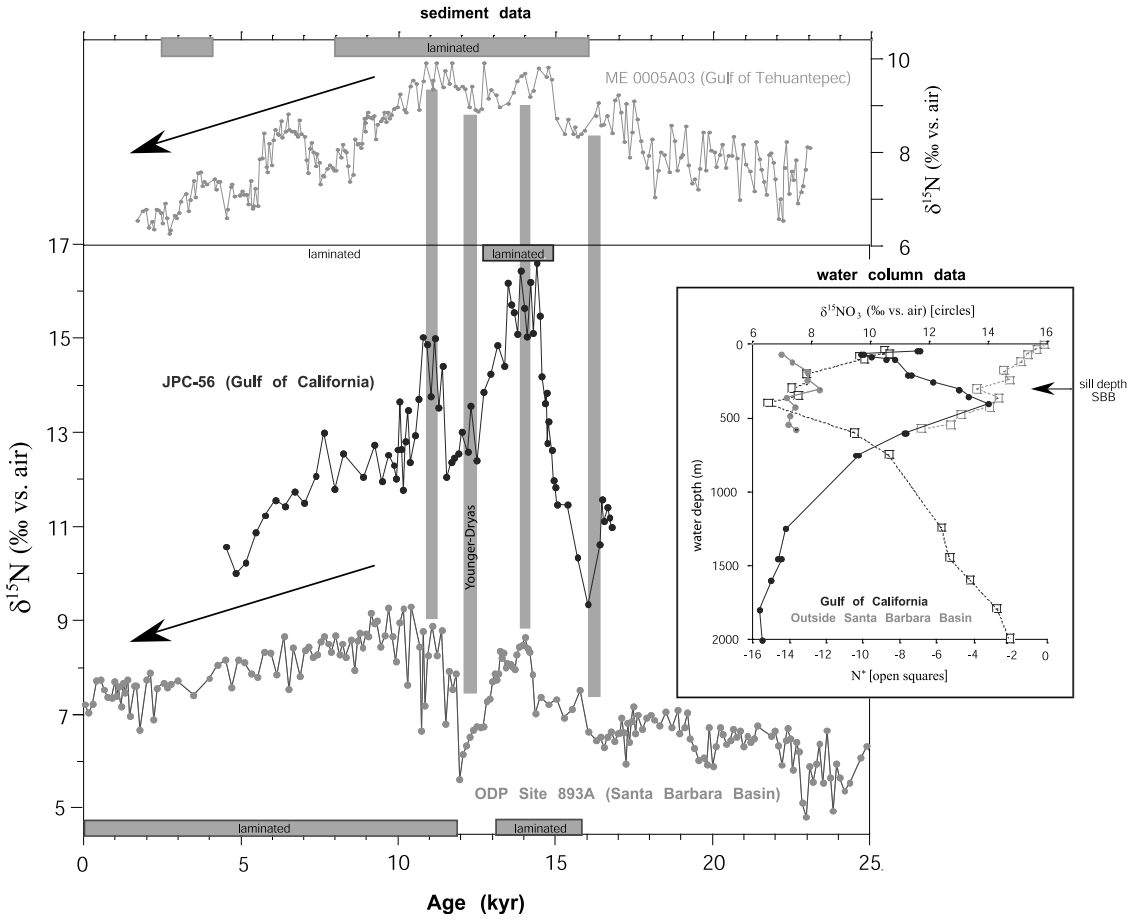

Figure 1. Downcore records of bulk sediment $\delta^{15}N$ from the eastern North Pacific (Gulf of Tehuantepec, Mexican margin [*Thunell and Kepple*, 2004]; Gulf of California [*Pride et al.*, 1999]; and Santa Barbara Basin [*Emmer and Thunell*, 2000]). Intervals of sediment lamination are indicated with a gray bar for each record. The Mexican margin and the Gulf of California are regions of active water column denitrification today, whereas the waters overlying the Santa Barbara Basin are influenced by the northward advection (in the California Undercurrent) of the denitrification signal from the south (nitrate $\delta^{15}N$ (solid circles) and N* (open squares) shown in inset [*Altabet et al.*, 1999; *Sigman et al.*, 2003]). See color version of this figure at back of this issue.

oceanic inventory of N on a timescale comparable to glacial/interglacial transitions (less than 10 kyr).

[4] Because the dominant sources and sinks in the N budget influence the $^{15}N/^{14}N$ of oceanic nitrate in distinct ways, the $^{15}N/^{14}N$ of organic N preserved in sediments offers the potential to reconstruct past changes in the N budget. While N isotope paleoceanography is in its infancy and there are few sediment $^{15}N/^{14}N$ records away from denitrification zones, there are several adequately robust observations that we use to guide this study. First, sediment $^{15}N/^{14}N$ is observed to increase upon deglaciation in regions of modern water column denitrification, suggesting that denitrification in the thermocline of these regions increased at the end of the last ice age [*Altabet et al.*, 2002; *Ganeshram et al.*, 2000]. Second, many of these same sediment records include a subsequent decrease in sediment $^{15}N/^{14}N$ through the early Holocene, with the amplitude of this decrease being similar to or smaller than the initial $^{15}N/^{14}N$ increase upon deglaciation (Figure 1). Third, records distant from denitrification zones suggest no significant change in sediment $^{15}N/^{14}N$ from Last Glacial Maximum to late Holocene, suggesting that mean ocean nitrate $^{15}N/^{14}N$ has not changed significantly between these two climate states [*Kienast*, 2000]. Fourth, and least certain, some of the records outside denitrification zones also suggest a deglacial/early Holocene $^{15}N/^{14}N$ maximum that is reminiscent of the deglacial maximum observed in the denitrification regions but of smaller amplitude [*Holmes et al.*, 1997; *Kienast*, 2000].

[5] The first of these observations provides clear evidence for significant climate-associated changes in the fixed N budget. Specifically, the deglacial increase in $^{15}N/^{14}N$ of organic N in sediments underlying the ocean's major suboxic zones imply that the rate and/or extent of water column denitrification (an ^{15}N-enriching process) was reduced during glacial periods [*Altabet et al.*, 1995; *Ganeshram et al.*, 1995]. The deglacial increase in water column denitrification was driven by a climate-related increase in the intensity and/or extent of thermocline suboxia [*Keigwin and Jones*,

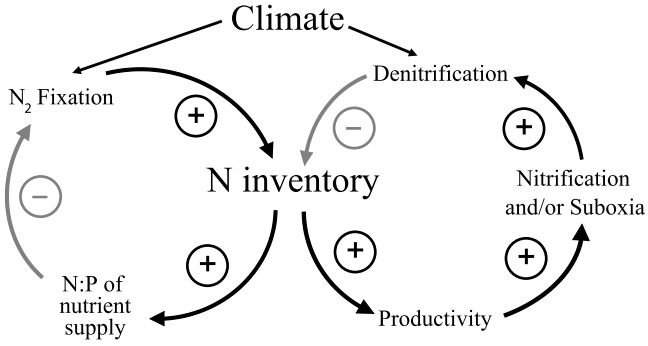

Figure 2. Schematic of previously hypothesized N budget feedbacks. Perturbations to the N inventory could be regulated through feedbacks by either denitrification (e.g., changes in the preformed nitrate concentration of the thermocline causing changes in low-latitude productivity, which affects the extent of suboxia and therefore denitrification) or N_2 fixation (changes in N inventory causing changes in the N:P of the nutrient supply to the surface ocean, which affects the competitive advantage of N_2 fixing organisms and therefore N_2 fixation). The denitrification negative feedback loop also works for benthic denitrification, which is not very sensitive to bottom water [O_2] but is sensitive to sediment nitrification rates and thus to the productivity-driven flux of organic matter to the sediments. Each step in the feedback mechanism involves a direct proportionality (arrow with plus sign) or an inverse proportionality (arrow with minus sign), but the sum of the processes in each case constitutes a negative feedback.

1990; *Kennett and Ingram*, 1995]. Other climate-associated changes in the N budget have also been proposed. *Christensen* [1994] argued that sedimentary denitrification was lower during glacial periods due to the reduced area of the continental shelf, where most sedimentary denitrification is thought to occur. Finally, *Falkowski* [1997] and *Broecker and Henderson* [1998] have proposed that the higher glacial dust flux recorded in ice cores relieved iron limitation of N_2 fixing cyanobacteria, thereby increasing glacial N_2 fixation and adding to the N imbalance resulting from denitrification changes.

[6] Each of these potential climate-forced changes in the N budget would contribute to a cycle of oceanic nitrate depletion during interglacials and nitrate accumulation during ice ages. Even if only water column denitrification changes during glacial cycles, the ocean would still undergo large changes in N inventory. A deglacial increase in water column denitrification of 60% (~40 TgN/yr), with all other fluxes remaining constant since the Last Glacial Maximum, would have removed 60×10^4 TgN, equivalent to the modern oceanic nitrate inventory, over the ensuing 15 kyr. Furthermore, if sedimentary denitrification also increased and/or N_2 fixation decreased into the Holocene [*Christensen*, 1994; *Falkowski*, 1997], then the N depletion would have been even faster.

[7] Glacial/interglacial swings in N inventory of these magnitudes would have dramatic impacts on oceanic productivity. Simple box models of the ocean suggest that changes in nutrient inventory cause roughly proportional changes in subtropical and tropical ocean productivity [*Broecker*, 1982a, 1982b; *Broecker and Peng*, 1987; *Sigman et al.*, 1998]. Yet, the geologic record provides no evidence of dramatic peaks or drops in global ocean productivity over glacial/interglacial cycles, or on longer periods [*Blunier et al.*, 2002]. Instead, the evidence suggests that the fertility of the ocean has been remarkably stable over thousands and millions of years (reviewed by *Sigman and Haug* [2003]).

[8] One way to reconcile the inferred climatically induced N budget perturbations with the apparent stability of oceanic productivity is to invoke the presence of negative feedbacks that regulate the N budget. Two such feedbacks have been proposed, one involving N_2 fixation [*Ganeshram et al.*, 2002; *Haug et al.*, 1998; *Redfield et al.*, 1963; *Tyrrell*, 1999], and the other involving denitrification [*Codispoti*, 1989; *Toggweiler and Carson*, 1995]. The N_2 fixation feedback hinges on a relationship between the $[NO_3^-]$:$[PO_4^{3-}]$ ratio of the ocean and the competitive advantage of N_2 fixing organisms [*Redfield et al.*, 1963; *Tyrrell*, 1999] (Figure 2). When N becomes depleted relative to P, the nutrient supply to the euphotic zone will lead to more N limitation. Organisms capable of using the excess P by fixing their own N would be expected to find an expanded ecological niche, and inputs of newly fixed N would increase, raising the N inventory. As the ocean's N and P approach the ratio needed by phytoplankton, the energetically costly process of N_2 fixation would be discouraged since N supply would be sufficient to use the available P.

[9] Feedbacks involving N sinks may also help to regulate the N inventory (Figure 2). For example, an increase in the nitrate reservoir would lead to an increase in the export of organic matter (assuming a flexible C:P ratio). This would cause an expansion of thermocline suboxia and therefore an increase in water column denitrification, which would work against the climatically forced increase in the nitrate reservoir. While sedimentary denitrification is not strongly coupled to suboxia in bottom waters [*Devol*, 1991], one would also expect it to increase with increasing export production and organic matter flux to sediments [*Christensen et al.*, 1987]. Thus sedimentary denitrification offers an additional negative feedback, although one might expect the strength of the sediment-related feedback to be somewhat weaker. The potential for glacial/interglacial changes in the N inventory depends on the combined strength of these negative feedbacks in their response to climate forcing of the N cycle.

[10] Different N budget feedbacks may be competitive, if not mutually exclusive. The more effectively any source/sink term counteracts perturbations to the N inventory, the smaller will be the effective perturbation to which other source/sink terms respond. For example, the N deficits generated by a deglacial increase in denitrification might be rapidly and completely compensated by an increase in N_2 fixation. If the N:P ratio of export production remains unchanged as a result, there will be no change in the flux of organic N through the suboxic layer, and the denitrification feedback would be irrelevant. On the other hand, if N_2 fixation responds only weakly to the N deficit, export production will decrease, and a denitrification feedback will be the dominant mechanism for stabilizing the N reservoir.

[11] The sensitivities of different feedbacks will combine with the strength of climate forcings to determine the change in each of the N budget fluxes. Since the dominant sources and sinks of oceanic fixed N all have different isotope effects, one might expect both the forcings and the feedbacks to be reflected in sediment N isotope records. The observations summarized above provide a basis for assessing the importance of forcing and feedback processes in N budget changes.

[12] Here we develop and apply a box model of the ocean N cycle designed to capture the processes most relevant to the isotopic composition of subsurface nitrate, the largest pool of fixed N in the ocean. We begin by exploring the factors that control the steady state $^{15}N/^{14}N$ ratio of nitrate. We then perform a series of simulations in which we assume a given deglacial forcing of the N cycle, specifically, a stepwise increase in water column denitrification upon deglaciation [*Altabet et al.*, 1995; *Ganeshram et al.*, 1995] and a more gradual deglacial increase in sediment denitrification that is paced by sea level rise [*Christensen*, 1994; *Bard et al.*, 1990]. These simulations include previously proposed feedbacks on the N budget, which are assessed by comparison with sediment $^{15}N/^{14}N$ records. This model is one step toward integrating these interactions in a way that allows us to test various hypotheses against the constraints provided by paleoceanographic data.

2. Model

[13] In this section, we develop a box model that represents, in a simplified manner, the relevant processes in the marine nitrogen cycle: N_2 fixation, sediment denitrification, water column denitrification, the tropical/subtropical biological pump, and water mass transport and mixing. We use the model to identify the factors that control the steady state isotopic composition of oceanic nitrate. The nitrate supply to the surface is fully consumed in most of the low-latitude ocean, so the $^{15}N/^{14}N$ of the sinking flux typically reflects that of the subsurface nitrate [*Altabet*, 1988; *Altabet et al.*, 1999; *Thunell et al.*, 2004].

2.1. Considerations

[14] A first approximation to the steady state mean ocean nitrate $^{15}N/^{14}N$ ratio can be understood by considering a homogeneous nitrate pool influenced by N_2 fixation and denitrification. At steady state, N_2 fixation (F) must balance water column denitrification (W) plus sedimentary (or benthic) denitrification (B). N_2 fixation supplies new fixed N from the large reservoir of atmospheric N_2 with little fractionation [*Carpenter et al.*, 1997], so we set the ^{15}N source to $R_a \times F$, where R_a is the $^{15}N/^{14}N$ ratio of atmospheric N_2. This must balance the loss of ^{15}N by water column and sedimentary denitrification, $(^{15}N/^{14}N) \times (\alpha_b B + \alpha_w W)$, where the α's are their respective fractionation factors.

[15] Water column denitrification expresses a strong preference for ^{14}N (we assume $\alpha_w = 0.975$) [*Barford et al.*, 1999], leaving behind ^{15}N-enriched nitrate [*Altabet et al.*, 1999; *Liu and Kaplan*, 1989; *Sigman et al.*, 2003; *Voss et al.*, 2001; *Brandes et al.*, 1998]. In contrast, sedimentary denitrification is thought to occur with little apparent isotopic fractionation ($\alpha_b = 1$), due to the effects of pore-water diffusion [*Brandes and Devol*, 1997; *Sigman and Casciotti*, 2001]. The steady state isotopic balance can be solved (with $F = W + B$) for the $^{15}N/^{14}N$ ratio

$$^{15}N/^{14}N = R_a \times (\alpha_b(1 - f_w) + \alpha_w f_w),$$

where the fraction of total denitrification occurring in the water column is denoted f_w ($f_w = W/(W + B)$) [*Brandes and Devol*, 2002]. Thus the steady state $^{15}N/^{14}N$ ratio (or $\delta^{15}N$, defined as $\delta^{15}N = ((^{15}N/^{14}N)_{sample}/(^{15}N/^{14}N)_{reference} - 1) \times 1000‰$, where the reference is atmospheric N_2) of a homogeneous ocean with N sinks of different fractionations depends only on the relative magnitude of those sinks (f_w) and their fractionation factors. If a given N_2 fixation source is balanced predominantly by water column denitrification ($f_w \rightarrow 1$), ^{14}N will be preferentially removed from the ocean, giving a high $\delta^{15}N$ for mean ocean nitrate. On the other hand, if most of the denitrification occurs in sediments ($f_w \rightarrow 0$) with little fractionation, the $\delta^{15}N$ ratio of the nitrate loss will be closer to that of mean ocean nitrate, so the $\delta^{15}N$ of oceanic nitrate will be low (approaching the input ratio, R_a).

[16] *Brandes and Devol* [2002] have compiled a N isotope budget for the Holocene ocean. They estimate that additional N sources from atmospheric deposition and rivers together are isotopically similar to N_2 fixation, while the additional sink due to organic N burial is isotopically similar to mean ocean nitrate (and in this way similar to sediment denitrification). Therefore these additional smaller budget terms do not significantly alter the conclusion based on N_2 fixation and denitrification alone that f_w is the dominant control on mean ocean nitrate $\delta^{15}N$.

[17] However, this homogeneous model of the mean $\delta^{15}N$ of ocean nitrate leaves out an important consideration. In the real ocean, water column denitrification is localized, so that nitrate loss occurs in nitrate pools with a $\delta^{15}N$ that is different from that of the mean ocean nitrate. As water column denitrification consumes nitrate in the suboxic water mass, it raises the $\delta^{15}N$ of the residual nitrate in the suboxic zone. However, because the nitrate $\delta^{15}N$ of a mixture of two water parcels is biased toward the parcel with higher nitrate concentration, the depletion of nitrate in the suboxic zone leads to a smaller isotopic influence of its residual nitrate on the ocean's mean $\delta^{15}N$ (Figure 3). In the limit of complete nitrate consumption within the suboxic zones of the ocean water column, the suboxic water mass acts only to dilute the nitrate concentration of the rest of the ocean, with no impact on its $\delta^{15}N$. In this limit, there would be no expression of the isotopic fractionation by water column denitrification [*Thunell et al.*, 2004]. Instead, it would be isotopically similar to sediment denitrification, and the sole dependence of mean ocean nitrate $\delta^{15}N$ on f_w would no longer hold. We refer to this as "the dilution effect." The dilution effect also results from decreasing total oceanic nitrate. As the mean ocean nitrate concentration decreases, a given amount of denitrification consumes a greater fraction of the nitrate in the suboxic zone, enriching the suboxic nitrate pool but decreasing its influence on the mean ocean $\delta^{15}N$ (Figure 3b).

[18] From these considerations it can be expected that increasing total denitrification ($B + W$) or decreasing the total nitrate reservoir in a steady state ocean with constant

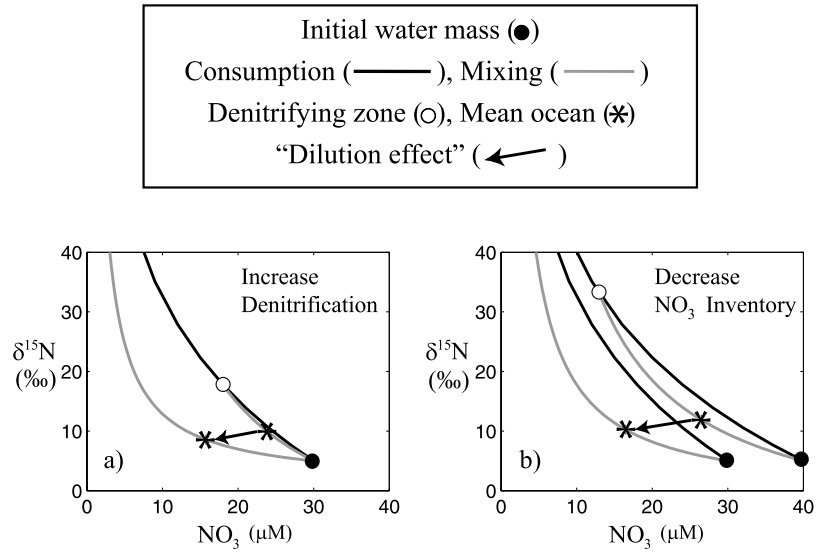

Figure 3. Illustration of the dilution effect for (a) increased denitrification and (b) decreased N inventory (or mean $[NO_3^-]$). As denitrification increases, the $\delta^{15}N$ of the denitrification zone (open circle) increases due to Rayleigh fractionation (dark curve). The mixture of denitrified water (open circle) and the rest of the ocean in its initial state (solid circle) falls along a mixing line (light curve) in which the $\delta^{15}N$ of the mixed water mass (star) is biased toward the end-member with high nitrate concentration. The decrease in mean $\delta^{15}N$ is a measure of the dilution effect (arrow). This effect is produced by either an increase in denitrification (Figure 3a) or a decrease in total nitrate (Figure 3b). Note that higher $\delta^{15}N$ values in the denitrification zone are extreme in these illustrative cases, and fall outside the plotted range.

f_w will increase the $\delta^{15}N$ of the suboxic zone while decreasing the $\delta^{15}N$ of the mean ocean nitrate pool. That is, for a given f_w, increased fractional nitrate consumption in the suboxic zone leads to greater nitrate ^{15}N-enrichment in that zone while reducing the ^{15}N-enrichment of mean ocean nitrate (Figure 3). In order to make reliable use of sediment records from both oxic and suboxic regions of the ocean, we therefore require a model that accounts for this spatial structure.

2.2. Model Structure

[19] In order to account for these potential spatial differences in nitrate $\delta^{15}N$, we construct a box model that divides the ocean horizontally into a suboxic water column and the rest of the ocean (Figure 4). We take the suboxic water column to be the areal extent of waters with annual mean O_2 concentrations below 10 μM in the NOAA NESDIS Atlas [*Conkright et al.*, 1994]. This definition includes the eastern tropical North and South Pacific and the Arabian Sea, and comprises ~2.5% of the global ocean area. The resolution of high-latitude processes has been shown to be a central concern for many paleoceanographic questions [e.g., *Sarmiento and Toggweiler*, 1984]. However, the focus of this study is the interaction between the suboxic water column and the adjacent waters. This is essentially a low-latitude phenomenon; therefore, we choose not to include the structure of high-latitude water masses in this box model.

[20] Both horizontal regions are divided into four vertical levels (Figure 5): a surface box (0–100 m) in which nitrate uptake and organic matter export occurs, and three lower boxes in which the organic N flux is remineralized with depth according to a power law (*Martin et al.* [1987], exponent = 0.858). In the suboxic water column, remineralization is deeper (exponent = 0.40), consistent with the findings of *Van Mooy et al.* [2002]. The depth of the lower thermocline box (275–800 m) is chosen to coincide with the depth of the climatological suboxic water volume (2×10^{14} m^3). The deep ocean is taken to be from 800 to 4000 m.

[21] The horizontal regions and depth levels are connected through lateral and vertical mixing and advection designed to represent the key features of ocean circulation that cause the major suboxic zones. Upwelling, which brings high-nutrient waters to the surface in the suboxic water column, stimulates high biological productivity and creates a high oxidant demand below the mixed layer. In addition, thermocline waters in these regions are generally poorly ventilated. These two features are incorporated in the model by adding to the mixing terms an upwelling flux in the suboxic water column (compensated by downwelling in the rest of the ocean), and by removing lateral mixing between the suboxic box and the lower thermocline of the rest of the ocean. The resulting pattern of mixing and transport is shown in Figure 5.

[22] Model water mass fluxes are calculated by fitting the steady state phosphate concentrations in the model to annual mean values [*Conkright et al.*, 1994]. We require vertical mixing rates to be the same in the suboxic water column and the rest of the ocean, on a per area basis. This leaves seven fluxes to solve for: three vertical mixing fluxes, three horizontal mixing fluxes, and the upwelling/downwelling flux. The least squares solution is found using the seven

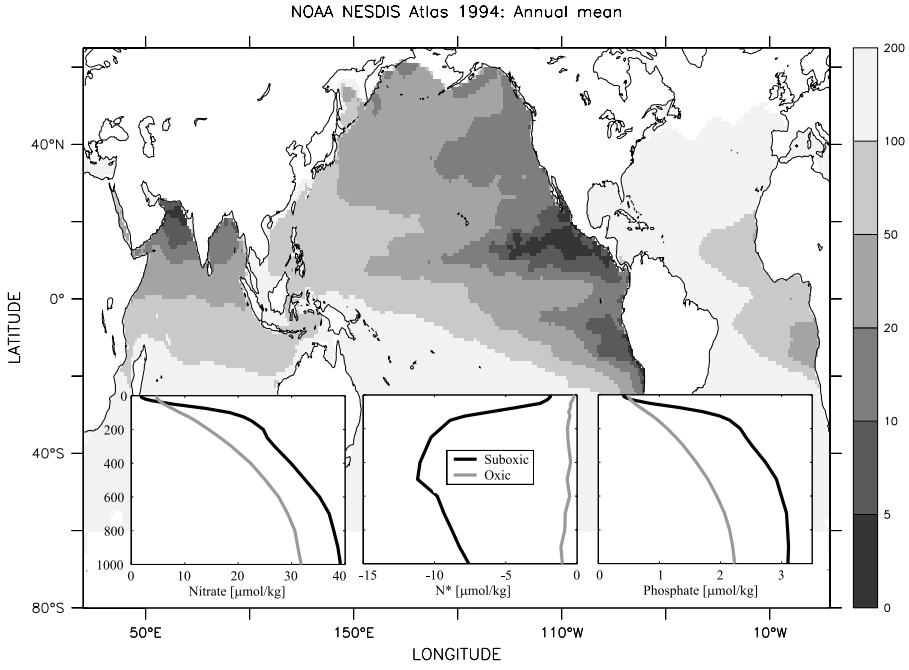

Figure 4. Map of O_2 concentration (μmol/kg) at the depth of the climatological O_2 minimum [*Conkright et al.*, 1994]. Insets: area-averaged nutrient profiles (NO_3^-, PO_4^{3-}, and N* = $[NO_3^-]$ − 16*$[PO_4^{3-}]$ + 2.9) from the suboxic water column (dark curves) and the rest of the ocean (light curves). The threshold for suboxia is taken to be $O_2 < 10$ μmol/kg so as to include the eastern tropical North and South Pacific and the Arabian Sea.

linearly independent box conservation equations (the eighth is not independent since it can be derived from total mass conservation).

[23] Export production is specified in the inverse solution. On the basis of GCM results, we specify a global organic matter export of 10 GtC/yr, with ∼10% occurring in the suboxic water column (about 4 times the areal mean export flux). The resulting vertical and horizontal mixing are high in near-surface waters, decreasing with depth (Figure 5). As with most box models, the magnitude of subsurface vertical mixing required to sustain a realistic export flux is quite high [*Matsumoto et al.*, 2002]. We could have chosen instead to require more realistic (lower) mixing and transport fluxes, at the expense of a realistic export flux. This choice changes only the absolute magnitudes of mass fluxes, not their relative magnitudes. We chose to have a realistic export flux because this will determine the absolute values of the N source/sink terms, which we wish to compare with other estimates.

[24] On the basis of these mass fluxes, the forward model can be written as a set of equations for N (nitrate), P (phosphate), and ^{15}N (^{15}N-labelled nitrate). In the *i*th box,

$$dP_i/dt = -\mathrm{Prod}(P_i) + \mathrm{Remin}(P_i) + \mathrm{Circ}(P_i),$$

$$dN_i/dt = -\mathrm{Prod}(N_i) + \mathrm{Remin}(N_i) + \mathrm{Circ}(N_i) + F_i - W_i - B_i,$$

$$d^{15}N_i/dt = -\mathrm{Prod}(^{15}N_i) + \mathrm{Remin}(^{15}N_i) + \mathrm{Circ}(^{15}N_i) + \alpha_f R_a F_i - \alpha_w R_i W_i - \alpha_b R_i B_i,$$

where "Prod" is the uptake of each component by biological production, "Remin" is the release of each component by organic matter remineralization, and "Circ" is the redistribution of each component due to ocean circulation. The sources and sinks of fixed N are denoted *F* (N_2 fixation), *W* (water column denitrification), and *B* (sediment, or "benthic," denitrification). The corresponding ^{15}N terms are multiplied by the $^{15}N/^{14}N$ ratio (*R*) of the source pool, as well as the isotope fractionation factors, α. We assume that N_2 fixation adds nitrate with the $^{15}N/^{14}N$ ratio of air (R_a) without fractionation ($\alpha_f = 1.0$) [*Carpenter et al.*, 1997]. In each box, denitrification removes nitrate with the local isotope ratio (R_i) modified by no isotope fractionation in the sediments ($\alpha_b = 1$) [*Brandes and Devol*, 1997] and 25‰ in the water column ($\alpha_w = 0.975$) [*Barford et al.*, 1999]. In the forward model, export production is calculated by restoring surface phosphate concentration toward annual mean observations. Production and remineralization fluxes of nitrate are calculated as 16 times phosphate fluxes.

[25] We neglect smaller terms in the N budget, such as atmospheric and riverine sources and the sink due to burial

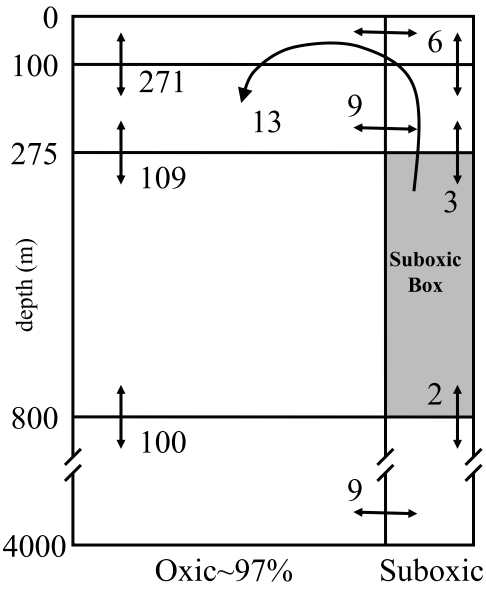

Figure 5. Schematic of model geometry and fluxes. The suboxic water column (~3% of ocean area) communicates with the rest of the ocean through horizontal mixing and an advective overturning flux (up in the suboxic water column, down in the oxic water column, and from oxic to suboxic below 800 m). Both water columns are divided into four levels (depths indicated at left) which are connected by vertical mixing and the upwelling/downwelling component of overturning. Water mass fluxes, given in Sverdrups (10^6 m^3 s^{-1}), are determined by matching the PO_4 distribution (see text).

in the sediments. These terms are not clearly isotopically distinct from the primary terms in the budget and are very poorly understood [*Brandes and Devol*, 2002]. We seek a minimal model here, avoiding complexities that would cloud the important processes.

[26] Water column denitrification in the model is confined to the suboxic box. Sediment denitrification is distributed between the suboxic water column and the rest of the ocean with equal rates per unit area. In the absence of detailed information about the vertical distribution of sedimentary denitrification, we apply 30% in the seafloor adjacent the top boxes [*Middelburg et al.*, 1996], 30% in the seafloor of both thermocline boxes, and the remaining 10% in the deep ocean. N_2 fixation flux follows export and remineralization terms, with 10% occurring in the suboxic water column. However, half of the newly fixed N is released in the surface ocean, while the remaining sinking flux is distributed with depth according to the Martin curve.

[27] The magnitude of the denitrification terms is tuned to fit two observed characteristics of the nitrate distribution. First, water column denitrification is chosen to match the N* gradient ($N^* = [NO_3^-] - 16^*[PO_4^{3-}] + 2.9$) in the suboxic water column. The magnitude of water column denitrification required is 70 TgN/yr, which is in the range of observational estimates [*Codispoti and Christensen*, 1985; *Deutsch et al.*, 2001]. The agreement between the model and observed values for this process suggests that total N supply to the suboxic box (via transport and remineralization) is roughly correct.

[28] Water column denitrification of this magnitude, balanced entirely by N_2 fixation, would yield a mean ocean isotopic composition of >16‰, well above the observed value of 5‰ [*Sigman et al.*, 2000] (although not 25‰, because of the dilution effect). In order to match the observed isotopic range, sediment denitrification of roughly 190 TgN/yr is required. This value lies between the older estimates based on in situ rate measurements [*Codispoti and Christensen*, 1985] and the upwardly revised estimates based on sediment modeling [*Middelburg et al.*, 1996] and on global isotopic mass balance considerations [*Brandes and Devol*, 2002]. Our estimate is methodologically most similar to that of *Brandes and Devol* [2002]. However, it is quantitatively lower, partially because we use a slightly smaller isotopic fractionation for sediment denitrification (α = 1.000 versus 0.9985), but mostly because our model includes the dilution effect described above.

[29] Modeled nitrate concentration, phosphate concentration, and N* agree with climatological values to within 5% on average (Figure 6). The suboxic water column has higher nutrient levels because the influx of nutrient-rich subsurface water is balanced by an outflow of relatively depleted surface water. Water column denitrification produces low N* in the suboxic zone, with strong gradients toward the surface. In contrast, the oxic water column N* is relatively uniform with depth in both the data and model.

[30] We compare model $\delta^{15}N$ for the suboxic and oxic water columns with data averaged over several profiles from the Eastern Tropical North Pacific [*Sigman et al.*, 2003] and the Sargasso Sea [*Karl et al.*, 2002; A. N. Knapp et al., The N Isotopic composition of dissolved organic nitrogen and nitrate at the Bermuda Atlantic Time-Series Study site, submitted to *Global Biogeochemical Cycles*, 2004], respectively. The model captures much of the observed spatial variability in nitrate $\delta^{15}N$ in the suboxic water column, similar to N* but with opposite sign. However, model nitrate $\delta^{15}N$ is consistently lower than the data by ~1.0‰ in this region. The upper thermocline of the suboxic zone in the model is too high in N* and too low in nitrate $\delta^{15}N$, probably because denitrification zones reach this depth in the real ocean. Because lateral mixing between the suboxic surface and the global surface is low, most of the surface-thermocline gradient of both N* and $\delta^{15}N$ in the suboxic water column is driven by N_2 fixation, as has been proposed on the basis of regional isotopic mass balance [*Brandes et al.*, 1998].

[31] The near-surface waters of the Sargasso Sea exhibit strong vertical $\delta^{15}N$ gradients, and these are not well captured by the model. The elevated $\delta^{15}N$ observed at the surface occurs because of isotopic fractionation by nitrate assimilation [*Sigman et al.*, 1999], a process not included in the model. This is relatively insignificant since nitrate is completely consumed in this region. More importantly, the low $\delta^{15}N$ of nitrate in the upper thermocline is lower in the Sargasso Sea data than in the model. This discrepancy may be due to the fact that the Sargasso Sea near Bermuda, where the nitrate $\delta^{15}N$ profiles were collected, deviates from the mean thermocline chemistry of the low- and mid-latitude ocean. The thermocline of the Sargasso Sea, which

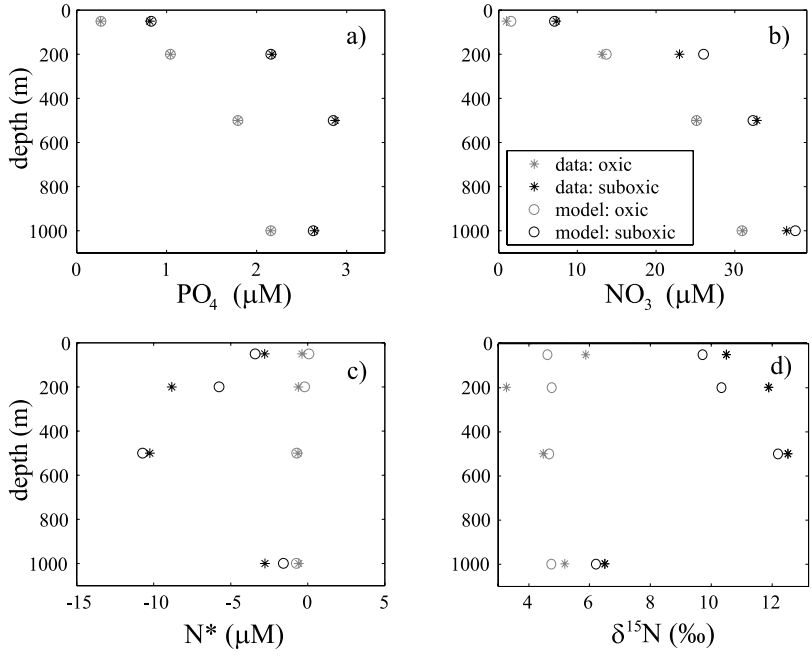

Figure 6. Profiles of model (circles) versus observed (stars) nitrate concentration, phosphate concentration, N*, and nitrate $\delta^{15}N$ in the suboxic water column (dark symbols) and the rest of the ocean (light symbols). Deep ocean properties are plotted shallower then their true average depth.

may be an area of intense N_2 fixation, is characterized by both high N* and low nitrate $\delta^{15}N$ [*Karl et al.*, 2002], and the global model does not resolve either of these features.

2.3. Deglacial Experiments

[32] We perform a series of simulations to investigate which climate-N cycle interactions most strongly determine the character of the nitrate isotopic evolution of the mean and suboxic water columns. We aim to identify possible glacial/interglacial scenarios that could explain the basic aspects of the glacial/interglacial records of sediment $\delta^{15}N$, in particular, the remarkable deglacial $\delta^{15}N$ maximum observed in many sites underlying or relatively near denitrifying regions. We include two direct forcings of climate change on the N cycle: a deglacial increase in water column denitrification caused by expanded interglacial suboxia [*Keigwin and Jones*, 1990; *Kennett and Ingram*, 1995] and a deglacial increase in sediment denitrification linked quantitatively to the observed timing of sea level rise [*Christensen*, 1994; *Bard et al.*, 1990]. We also include feedback processes that damp perturbations to the N budget.

[33] Each flux can be written as the product of its modern value and a time-dependent scaling factor that parameterizes the forcings and feedbacks,

$$W(t) = W_m \times \left(S_w + \alpha \frac{N(t) - \mathrm{N_o}}{\mathrm{N_o}} + \lambda H(t) \right),$$

$$B(t) = B_m \times \left(S_b + \beta \frac{N(t) - \mathrm{N_o}}{\mathrm{N_o}} + \varphi L(t) \right),$$

$$F(t) = F_m \times \left(S_f + \gamma \frac{N(t) - \mathrm{N_o}}{\mathrm{N_o}} \right).$$

The *m*-subscripted terms are the modern values of water column denitrification, sediment denitrification, and N_2 fixation, determined in the previous section. The first scaling terms, denoted by *S*, are constants that convert the modern fluxes to glacial initial values (see below). The second scaling terms represent N cycle feedbacks. The fraction $(N(t) - N_o)/N_o$ is the change in the N inventory, $N(t)$, relative to its initial glacial value, N_o. The fractional change in N inventory causes changes in fluxes through sensitivity factors α, β and γ. The functions $L(t)$ and $H(t)$ represent the forcing of sedimentary and water column denitrification by sea level rise and suboxia changes, respectively (*L* for "level", *H* for "hydrographic"). These functions take on values between 0 and 1, so that φ and λ are the maximum fractional changes in sedimentary and water column denitrification driven by these processes.

[34] While the feedbacks included here are intended to represent those discussed in the introduction, the feedback mechanisms themselves are not explicitly modeled. For example, we are not modeling O_2 concentrations or the competitive advantage of N_2 fixers. Instead, changes in N fluxes are linked directly to the N inventory such that the net effect of all the implicit steps in each feedback is represented by a single sensitivity parameter. The feedback terms are constructed so that a 1% increase in global N inventory causes an α % increase in *W*, a β % increase in *B*, and a γ % decrease in *F*.

[35] The fraction of glacial/interglacial sea level rise, $L(t)$, ranges from 0 at the Last Glacial Maximum to 1 at the present time. We fit (by eye) a hyperbolic tangent to sea level reconstruction data from *Bard et al.* [1990] and *Hanebuth et al.* [2000] (Figure 7). Sea level rise begins

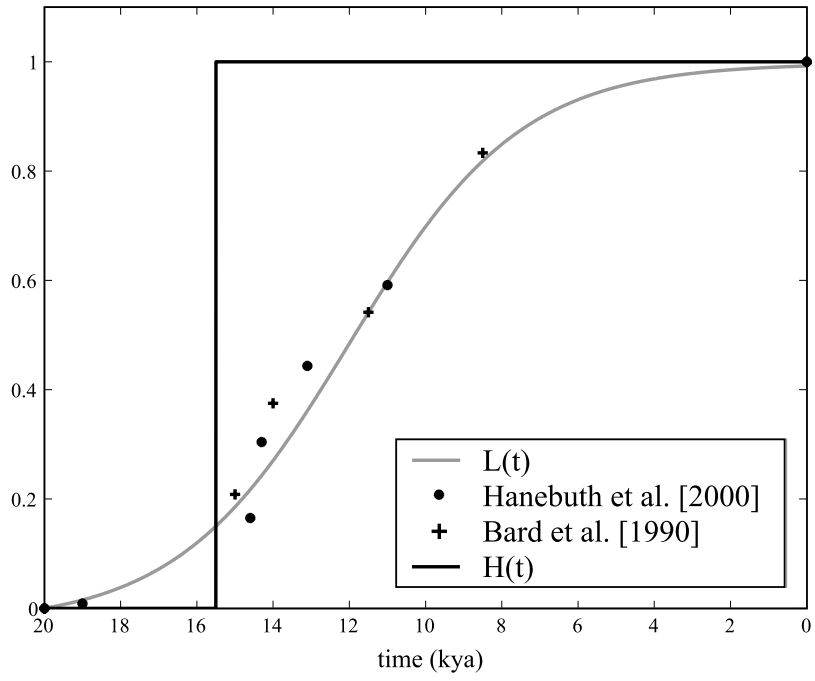

Figure 7. Water column denitrification and sea level rise forcing functions, $H(t)$ (dark curve) and $L(t)$ (light curve), as a fraction of their glacial-to-interglacial change (see text). Relative sea level rise is computed by fitting a hyperbolic tangent to the reconstruction data of *Bard et al.* [1990] and *Hanebuth et al.* [2000]. Water column denitrification increase is assumed to occur at the onset of laminations (~15 kya) in the eastern tropical Pacific [*Keigwin and Jones*, 1990].

slowly at the onset of deglaciation 20,000 years ago, reaching only 10% of its glacial/interglacial change after ~4000 years. In contrast, we assume that the deglacial onset of suboxia is rapid, so that a step function, $H(t)$, is appropriate (Figure 7). Many proxy records of suboxia from the eastern tropical Pacific date its onset at ~15 kya, with a brief return to oxic conditions between 12.9 and 11.6 kya in some areas during the Younger-Dryas [*Keigwin and Jones*, 1990; *Zheng et al.*, 2000]. The Younger-Dryas interval inferred from the sea level reconstruction [*Bard et al.*, 1990] is coincident with that inferred from sediment laminations [*Keigwin and Jones*, 1990], suggesting that the timing of our two climate forcings are consistent. Because the Younger-Dryas appears to influence the sediment $\delta^{15}N$ in some locations (see Figure 1), we tested the impact of including a brief return to oxic conditions during the Younger-Dryas in the forcing, $H(t)$. While the experiments with more detailed forcing were better able to reproduce short-term features associated with the Younger-Dryas in some sediment cores, the basic trends in glacial/Holocene $\delta^{15}N$ were not changed. Since our primary purpose is to elucidate basic processes, rather than to simulate detailed sedimentary records, we represent the onset of interglacial suboxia as a single step change in the results that follow.

[36] The magnitude of forced deglacial denitrification increases in the sediments and water column are unknown. In order to determine a reasonable magnitude of water column denitrification forcing (i.e., λ), we examined the sensitivity of the deglacial increase in $\delta^{15}N$ in the model's suboxic surface waters to the initial increase in water column denitrification. We find that $\delta^{15}N$ increases are most realistic when water column denitrification increases by ~60% upon deglaciation. We therefore adopt a λ value of 0.6. For the impact of sea level rise on sedimentary denitrification, we examine two different forcing magnitudes. In a first set of experiments, we assume that forced denitrification increases in the water column and the sediments are of the same magnitude, so that $\lambda = \varphi = 0.6$. In a second set of experiments, we assume that the climate forcing of sedimentary denitrification is reduced relative to water column forcing. If glacial sediment denitrification was reduced only on the continental shelves, whose area was 75% lower during glacial periods [*Christensen et al.*, 1987], and if ~40% of modern sediment denitrification occurs on continental shelves [*Middelburg et al.*, 1996], then total sedimentary denitrification would have increased by only ~30% due to sea level rise. We therefore secondarily examine climate forcings in which $\varphi = 0.3$ and $\lambda = 0.6$.

[37] Finally, we note that the time evolution of each flux and the N inventory will depend on all of the feedback and forcing parameters. Specifically, although the climate forcing terms are prescribed, the evolution of each flux will depend on all of the feedbacks as well as the climate forcing. For any complete set of parameter values (α, β, γ, λ, and φ), a unique set of initial values for N inventory, sources, and sinks can be found for which the model will reach modern values 20,000 years after the onset of deglaciation. In other words, the glacial conditions (i.e., the scaling constants S_f, S_b, and S_w) for any model scenario are determined by the values of the forcing and feedback

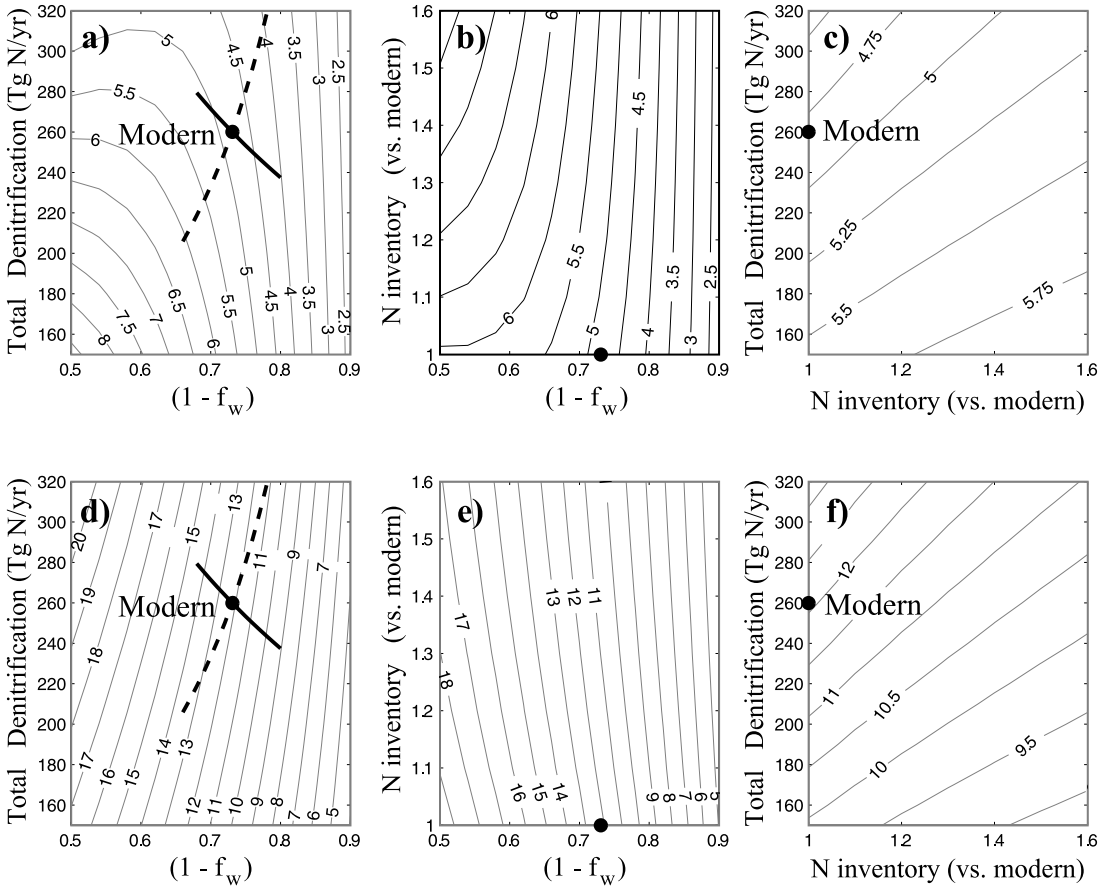

Figure 8. Steady state nitrate $\delta^{15}N$ contoured as a function of f_w (the fraction of total denitrification occurring in the water column), N inventory (relative to modern), and total denitrification for the (a–c) mean ocean and (d–f) suboxic zone. In both oceanic regions, f_w is the dominant control on $\delta^{15}N$ of nitrate (Figures 8a, 8b, 8d, and 8e). Total denitrification is a secondary factor (Figures 8a and 8d) as is N inventory (Figures 8b and 8e), though these have opposite effects in the mean and suboxic ocean. The effects of decreasing N inventory and increasing total denitrification (with f_w constant) are comparable in magnitude (Figures 8c and 8f), causing increases in $\delta^{15}N$ in the mean ocean and decreases in the suboxic zone. Bold lines in Figures 8a and 8d show the paths for changes in water column denitrification only (solid lines) and sedimentary denitrification only (dashed lines). Denitrification is shown in units of TgN/yr (1 TgN = 10^{12} grams N).

parameters. We perform simulations of the glacial/interglacial transition for all combinations of sensitivity parameters with values 0 (no feedback), 1 (weak feedback), and 9 (strong feedback).

3. Results

3.1. Controls on Ocean Nitrate $\delta^{15}N$ at Steady State

[38] Using this model, we quantify the deviation of the steady state mean $\delta^{15}N$ of ocean nitrate from the behavior expected in a homogeneous ocean (Figure 8). To do this, we compute the steady state nitrate $\delta^{15}N$ in each box for a range of values of sediment denitrification, water column denitrification, and N inventory. The $\delta^{15}N$ of nitrate for the mean ocean and the suboxic zone are shown (Figure 8). We plot these results as a function of the total denitrification rate and the fraction of total denitrification that occurs in the water column ("f_w") in order to more easily compare the results of the box model to those of the homogenous ocean (see section 2.1). For reference, trajectories of constant sedimentary and water column denitrification, an equivalent coordinate pair, are also shown with solid and dashed curves respectively.

[39] As observed in a homogenous ocean [*Brandes and Devol*, 2002], the dominant control on mean ocean nitrate $\delta^{15}N$ is f_w. This is a homogenous effect, causing $\delta^{15}N$ changes of the same sign in both the mean ocean nitrate (Figure 8a) and the nitrate found in the denitrifying region (Figure 8d). A secondary but significant dependence on total denitrification rate (for a given f_w) is also observed. This dependence is due to the "dilution effect" (see section 2.1) and is of opposite sign for the $\delta^{15}N$ of mean ocean and suboxic zone nitrate, producing contours of opposite slope in Figure 8a versus Figure 8d. An increase in total denitrification rate leads to greater nitrate consumption in the suboxic zone and thus greater ^{15}N enrichment of its residual nitrate

(Figure 8d). However, the higher degree of nitrate consumption in the suboxic zone means that the nitrate mixing out of that region has less impact on the mean ocean nitrate $\delta^{15}N$, so that increasing the denitrification rate (in steady state) causes a decrease in mean ocean nitrate $\delta^{15}N$ (Figure 8a). The effect of increasing water column denitrification alone can be seen by following the (solid) line of constant sedimentary denitrification toward the upper left. As water column denitrification increases, the $\delta^{15}N$ of mean ocean nitrate also increases, due to the ^{15}N enrichment. However, since the suboxic zone nitrate consumption is greater at higher water column denitrification rates, the dilution effect becomes stronger, and further increases in water column denitrification eventually begin to lower the mean ocean nitrate $\delta^{15}N$.

[40] There is a related secondary dependence on the mean ocean nitrate, again due to the dilution effect. With more nitrate in the ocean, a given denitrification rate consumes a smaller fraction of the nitrate that is transported into the suboxic region, leading to less ^{15}N enrichment of suboxic zone nitrate (Figure 8e). In the mean ocean, however, this causes the suboxic zone nitrate to make a greater contribution, so that mean ocean nitrate $\delta^{15}N$ is higher for a larger nitrate reservoir, approaching the solution for a homogenous ocean (Figure 8b). Nitrate inventory and total denitrification changes of the same relative magnitude elicit the dilution effect nearly equally (Figure 8c).

[41] While the influence of the dilution effect on mean ocean $\delta^{15}N$ is modest compared to f_w, the dilution effect has two important implications. First, equilibrium changes in N inventory and/or total denitrification flux (with f_w constant) of ~50% are capable of causing changes in the $\delta^{15}N$ of the suboxic zone and mean ocean nitrate of >2‰ and >0.5‰, respectively (Figures 8c and 8f). Isotopic changes of these magnitudes are significant in comparison to observed changes, so that the dilution effect should be accounted for when considering glacial/interglacial changes in the N budget. For example, a glacial ocean with the same average nitrate $\delta^{15}N$ as the modern ocean [*Kienast*, 2000] but with a 30% higher mean nitrate and a 30% lower total denitrification rate would require a 10% lower f_w.

[42] Second, for a given magnitude of water column denitrification, small changes in f_w (when $f_w < 0.5$) imply large changes in sedimentary denitrification (Figure 8a, dashed line). In the homogeneous approximation, a mean ocean $\delta^{15}N$ of 5‰ implies that 80% of denitrification occurs in the water column. The dilution effect reduces this value only slightly, to ~70%, but the accompanying change in sedimentary denitrification is large, ~90 TgN/yr. This explains why our estimate for sedimentary denitrification is lower than that of *Brandes and Devol* [2002].

3.2. Deglaciation Experiments

[43] In the deglacial experiments, the transient evolution of nitrate $\delta^{15}N$ has two components. The first component arises from changes in the steady state isotopic composition. As the factors that control the steady state isotopic composition change, the $\delta^{15}N$ of the ocean changes in response. According to the steady state theory, this will occur by changing (1) the ratio of water column to sediment denitrification ("f_w"), (2) the size of the oceanic nitrate reservoir, or (3) the total denitrification rate (see section 3.1). Given the dominance of f_w in governing the steady state $\delta^{15}N$ of nitrate, it can be expected that a transient deglacial maximum in f_w will tend to produce a deglacial $\delta^{15}N$ maximum. The forcing adopted here, which includes a delay between increased water column denitrification (an f_w increase) and the bulk of sea level rise (an f_w decrease), contributes to an f_w maximum, and is therefore an important driver of a $\delta^{15}N$ maximum. However, the full isotopic response is also determined by the strength of the feedbacks, through both their ability to modify the evolution of f_w and their influence on changes in total nitrate and denitrification (i.e., the dilution effect).

[44] Second, $\delta^{15}N$ changes are also caused by imbalances in the N budget. N_2 fixation adds nitrate with a low $^{15}N/^{14}N$ ratio, so that an excess of this source causes mean ocean nitrate $\delta^{15}N$ to decrease, while an excess of denitrification preferentially consumes ^{14}N, raising the mean ocean nitrate $\delta^{15}N$. The deglaciation scenarios presented here all involve temporary imbalances in the N budget, in which deglacial climate forcing induces an excess of denitrification that is subsequently compensated by an increase in N_2 fixation, and/or a decrease in denitrification. While these temporary N budget imbalances contribute to isotopic changes, the evolution of mean ocean and suboxic nitrate $\delta^{15}N$ in each of these experiments can be understood largely on the basis of the factors controlling the steady state isotopic composition.

[45] For each scenario, an overall feedback strength may be defined as a weighted sum of the feedback sensitivities ($\alpha W + \beta B + \gamma F$). For a given forcing of the N budget, the glacial-to-interglacial nitrate loss depends on the overall feedback strength. The greater the overall feedback strength in the experiment, the smaller the deglacial decrease in the nitrate reservoir. Since changes in the nitrate reservoir are one of the factors controlling steady state nitrate $\delta^{15}N$, we divide our results into scenarios with weak and strong overall feedback strengths.

3.2.1. Deglacial Experiments With Equal Forcings and Weak Feedbacks

[46] Figure 9 includes five scenarios with equal denitrification forcings ($\phi = \lambda = 0.6$), and weak overall feedback strength. In each scenario, each feedback is either inoperative, with a sensitivity parameter (α, β, or γ) of 0, or weakly operative with a sensitivity parameter of 1. The simulations include one scenario with all feedbacks weakly operative $\alpha = \beta = \gamma = 1$), three scenarios with two feedbacks on and one feedback off, and a fifth scenario with N_2 fixation feedback only ($\alpha = \beta = 0$, $\gamma = 1$).

[47] In scenarios with a water column denitrification feedback, the water column denitrification rate decreases from its maximum at the onset of deglaciation but remains above its glacial level through the Holocene (Figure 9c). The difference in water column denitrification between the glacial and Holocene periods depends on the strength of the water column denitrification feedback compared to the strength of the other feedbacks. When there is no feedback on water column denitrification, there is no decrease in this flux following the deglacial rise, and the glacial/Holocene difference is largest (equal to the imposed 60% forcing). When the water column denitrification feed-

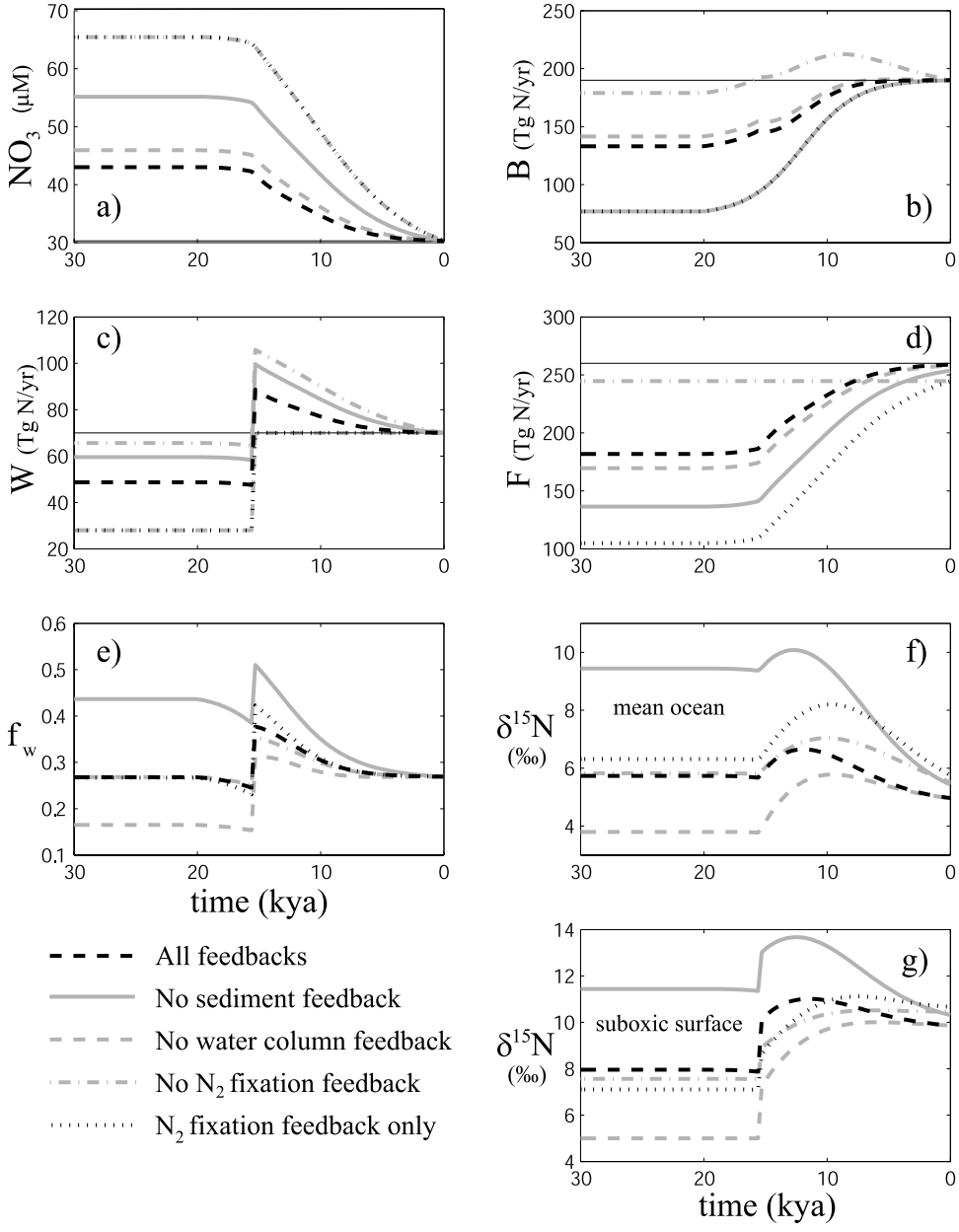

Figure 9. Time series of key variables in five scenarios with equal forcing of sediment and water column denitrification ($\lambda = \varphi = 0.6$) and weak overall N budget feedback. Variables are (a) mean ocean nitrate concentration ($[NO_3^-]$), (b) sedimentary denitrification (B), (c) water column denitrification (W), (d) N_2 fixation (F), (e) fraction of total denitrification occurring in the water column (f_w), (f) $\delta^{15}N$ for the surface box of the suboxic water column, and (g) mean ocean $\delta^{15}N$. Five model scenarios with weak overall feedbacks are shown: (1) all feedbacks on ($\alpha = \beta = \gamma = 1$; black dashed line (black in color version)), (2) no sedimentary denitrification feedback ($\alpha = 1$, $\beta = 0$, $\gamma = 1$; gray solid line (blue in color version)), (3) no water column denitrification feedback ($\alpha = 0$, $\beta = \gamma = 1$; gray dashed line (red in color version)), (4) no N_2 fixation feedback ($\alpha = \beta = 1$, $\gamma = 0$; gray dash-dotted line (green in color version)), and (5) N_2 fixation feedback only ($\alpha = \beta = 0$, $\gamma = 1$; black dotted line (pink in color version)). Each experiment is run for 30,000 years, starting from a glacial steady state that is determined by requiring N inventory and denitrification fluxes to reach modern values (thin black lines) at the end of the simulation. See color version of this figure at back of this issue.

back is operative, but overall feedback is weak (no N_2 fixation feedback), the decrease in water column denitrification following deglaciation must be relatively large in order to stabilize the rapidly decreasing N inventory, and the glacial/Holocene difference is small. N_2 fixation increases steadily, except where the N_2 fixation feedback is inoperative (Figure 9d). The increase is most pronounced where the N_2 fixation feedback alone responds to the deglacial denitrification forcing, leading to the largest glacial/Holocene difference in this flux.

[48] Sediment denitrification shows more complex behavior (Figure 9b). In all cases, there is an initial increase due to sea level rise. For a brief period following the forced increase in water column denitrification (~15 kya), the sediment denitrification feedback balances the impact of sea level rise, and sediment denitrification stabilizes. When there is no N_2 fixation response, nitrate losses are strongly compensated by the denitrification feedbacks, causing both denitrification terms to decrease gradually during the Holocene. In this case, the imposed (sea level-paced) sediment denitrification increase is roughly balanced by the sediment denitrification feedback, and the imposed deglacial increase in water column denitrification is roughly balanced by its feedback, so that both denitrification fluxes return to approximately glacial levels.

[49] All experiments show deglacial ^{15}N enrichments throughout the ocean due to the increase of water column denitrification (Figures 9f and 9g). The rise in nitrate $\delta^{15}N$ is strongest in the suboxic box (4–6‰, not shown), decreasing away from the denitrifying zone. Increases in suboxic zone nitrate $\delta^{15}N$ are communicated by vertical mixing and upwelling to the surface of the suboxic water column (Figure 9g), where they would be recorded by the formation and sinking of organic matter to the sediments [*Altabet et al.*, 1999]. Increases in $\delta^{15}N$ in the surface waters of the suboxic water column (hereafter "suboxic surface") range from 2 to 5‰ among the scenarios, with the largest increases occurring where the overall feedback is weakest (denitrification feedbacks or N_2 fixation feedback only).

[50] Subsequent to the deglacial $\delta^{15}N$ rise, all scenarios also reveal a decline in nitrate $\delta^{15}N$ throughout the ocean beginning in the late deglacial or early Holocene. The amplitude of this decrease varies considerably among the scenarios. The largest decreases in suboxic surface $\delta^{15}N$ occur in the scenario without sediment denitrification feedback (>3‰) or when all feedbacks are operative (>1‰). The remaining scenarios show minor decreases (<0.5‰). The case without sediment denitrification feedback undergoes the strongest deglacial decrease in the fraction of water column denitrification. It also exhibits the largest decrease in suboxic and mean ocean nitrate $\delta^{15}N$. Similarly, the scenario without water column denitrification feedback has the smallest decline in both f_w and nitrate $\delta^{15}N$. When all feedbacks are operative, the f_w and $\delta^{15}N$ curves lie between these two extremes. The relative magnitude and direction of nitrate $\delta^{15}N$ change in these three scenarios can be understood simply by considering the evolution of f_w.

[51] However, the remaining two scenarios, one with the N_2 fixation feedback only and the other with denitrification feedbacks only, have very similar f_w curves to the case with all feedbacks, and yet the suboxic $\delta^{15}N$ time series for these scenarios differ significantly. In these cases, the Holocene $\delta^{15}N$ decrease in the surface waters of the suboxic water column is very slight (0.1–0.3‰), beginning 7–8 kya, whereas in the case with all feedbacks operative, there is a stronger $\delta^{15}N$ decline (>1‰) beginning earlier (~12 kya). The similarity between the f_w curves in these scenarios indicates that the significant isotopic differences between them cannot be accounted for by f_w alone.

[52] The two scenarios which include feedbacks in either only the source flux (N_2 fixation) or only sink fluxes (denitrification) have the weakest overall feedback strength and therefore exhibit the largest glacial/interglacial loss of oceanic nitrate (Figure 9a). The greater total nitrate loss causes a given water column denitrification rate to consume a larger fraction of the nitrate supply to the suboxic zone, yielding greater local ^{15}N enrichment. Therefore, even while f_w returns toward its glacial value and mean ocean nitrate $\delta^{15}N$ decreases, the $\delta^{15}N$ in the suboxic water column remains nearly constant (Figure 10a). At the same time, the decreasing nitrate concentration of the suboxic zone reduces its influence on the $\delta^{15}N$ of mean ocean nitrate, causing mean ocean $\delta^{15}N$ to decrease more, relative to its initial increase, than does f_w. In other words, the sustained nitrate loss into the Holocene causes the suboxic $\delta^{15}N$ maximum to be less pronounced than the f_w maximum, and to diverge from the mean ocean $\delta^{15}N$ trend, which decreases more during the Holocene than would be expected solely on the basis of f_w.

[53] This stands in contrast to the scenario with all feedbacks weakly operative (Figure 10b), in which the nitrate $\delta^{15}N$ of the suboxic zone closely follows that of the mean ocean because the degree of nitrate consumption in the suboxic zone stabilizes in the early deglacial period. Reduced nitrate loss can also be obtained with the same f_w trajectory by increasing the strength of N_2 fixation feedback (Figure 10c). Thus, when feedbacks are weak, N imbalances persist longer and lead to larger total N losses. This causes the suboxic $\delta^{15}N$ rise to last longer and to have a larger magnitude, reducing the eventual Holocene decrease in suboxic zone nitrate $\delta^{15}N$ relative to cases with less global ocean nitrate loss.

[54] Of the scenarios presented so far, only the case with all feedbacks operative exhibits a deglacial maximum in suboxic zone nitrate $\delta^{15}N$ that fits the fundamental pattern observed in sediment $\delta^{15}N$ records from suboxic regions. However, the response of the mean ocean in this scenario offers an additional constraint. Despite identical f_w values in the glacial and Holocene, the dilution effect causes significant glacial/interglacial changes in mean ocean nitrate $\delta^{15}N$. The scenario with all feedbacks weakly operative undergoes a ~30% increase in total denitrification and a ~40% increase in nitrate inventory, with a change in mean ocean nitrate $\delta^{15}N$ of >1‰ between steady state glacial and interglacial periods. The data currently available do not support such a large change [*Francois et al.*, 1997; *Kienast*, 2000].

[55] In summary, among all of the scenarios with weak overall feedback (α, β, γ not greater than 1), none produces isotopic trajectories that agree with the available data for both the mean ocean and the suboxic regions. Scenarios in

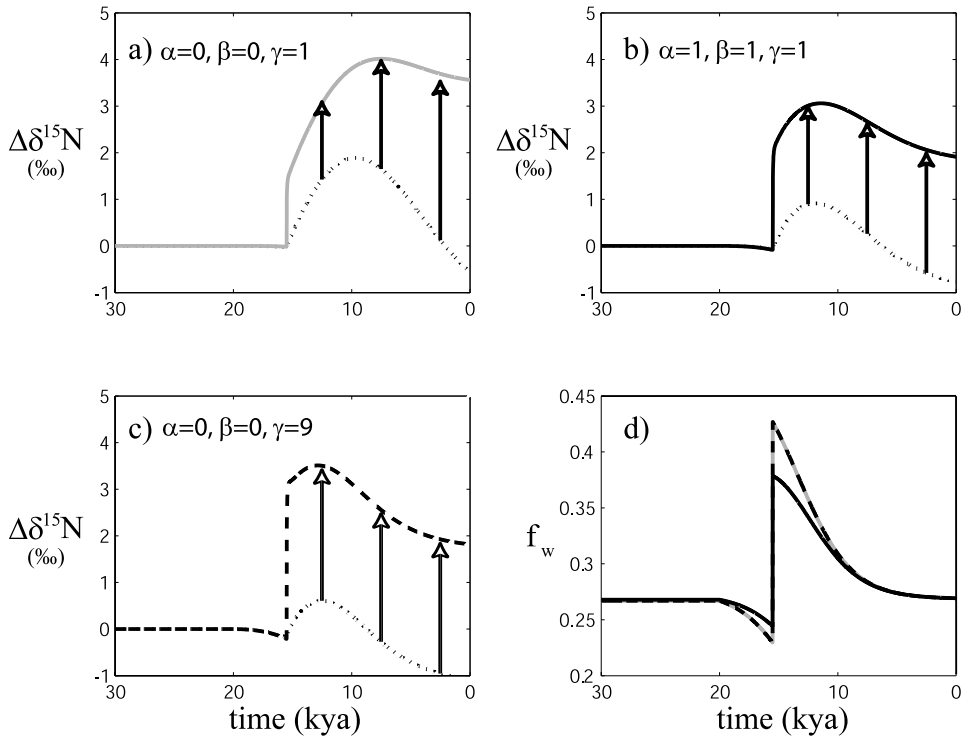

Figure 10. Changes in nitrate $\delta^{15}N$ in the mean ocean (dotted lines) and surface waters, overlying the suboxic zone for three scenarios, each with $\lambda = \varphi = 0.6$: (a) weak N_2 fixation feedback only ($\alpha = \beta = 0$; $\gamma = 1$, gray solid line (red in color version)), (b) all feedbacks operative but weak ($\alpha = \beta = 1$; $\gamma = 1$, black solid line (blue in color version)), and (c) strong N_2 fixation feedback only ($\alpha = \beta = 0$; $\gamma = 9$, black dashed line (green in color version)). (d) The fraction of denitrification occurring in the water column, f_w, is roughly the same in all cases. The differences in isotopic evolution of the mean ocean versus surface waters overlying the suboxic zone are due to nitrate consumption in the suboxic zone. Increased consumption of suboxic N throughout the Holocene leads to the divergence between mean ocean and suboxic $\delta^{15}N$ (Figure 10a), causing larger suboxic $\delta^{15}N$ increases and smaller subsequent decreases. See color version of this figure at back of this issue.

which the sensitivities of the sediment and water column denitrification feedbacks differ, exhibit significant glacial/interglacial differences in f_w, causing decreases in suboxic zone and mean ocean $\delta^{15}N$ that are too large or too small relative to observations. When the sediment denitrification feedback is off, lower interglacial f_w produces too large a Holocene decrease in nitrate $\delta^{15}N$. When the water column denitrification feedback is off, the Holocene f_w decrease is small, resulting in too little $\delta^{15}N$ decrease. In the scenarios in which both denitrification sensitivities are the same, f_w returns to its glacial value, but because overall feedback is weak, the continued loss of nitrate during the Holocene reduces the degree of Holocene nitrate $\delta^{15}N$ decline in the suboxic zone and/or causes too large a decrease in mean ocean nitrate $\delta^{15}N$ through the dilution effect. Thus the scenarios presented above fail to reproduce the basic character of observed $\delta^{15}N$ trends either because glacial/interglacial f_w changes are too large, or because the dilution effect is too strong due to weak feedbacks.

3.2.2. Deglacial Experiments With Equal Forcings and Strong Feedbacks

[56] Given the failure of deglacial scenarios with weak overall feedback, we examine three scenarios with stronger feedbacks, in which the effect of a continuously decreasing nitrate reservoir is reduced (Figure 11). The first scenario has a strong sediment denitrification feedback ($\beta = 9$) and a weak water column denitrification feedback ($\alpha = 1$), while the second scenario has the opposite feedback sensitivities. The third scenario has strong feedbacks for both denitrification terms ($\alpha = \beta = 9$). In all cases, the N_2 fixation feedback sensitivity is low ($\gamma = 1$).

[57] In the first scenario ($\alpha = 1$, $\beta = 9$, $\gamma = 1$), the strong sediment denitrification feedback compensates for most of the sea level forcing, causing this flux to remain roughly constant throughout the simulation. The feedback on water column denitrification is relatively weak, so that it decreases very little following its deglacial rise. The resulting time series of f_w shows a rapid increase upon deglaciation with little decrease thereafter. In the second scenario ($\alpha = 9$, $\beta = 1$, $\gamma = 1$), the water column denitrification feedback compensates for much of the deglacial nitrate loss, with a large reduction in this flux following its initial increase. Sedimentary denitrification increases close to its sea level-paced forcing, owing to a weak feedback for that flux. This leads to a large reduction in f_w following deglaciation, with modern values below those of the glacial period. When

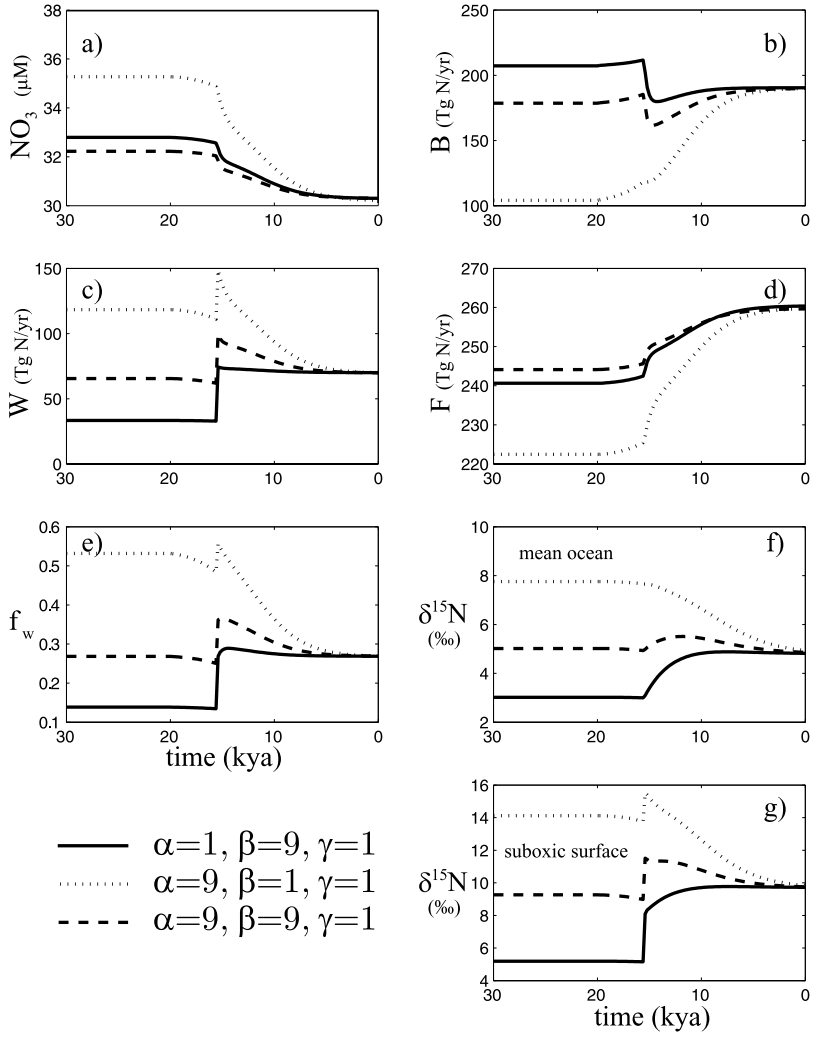

Figure 11. Same as Figure 9, but for three scenarios with strong feedbacks: (1) strong sedimentary denitrification feedback ($\alpha = 1$, $\beta = 9$, $\gamma = 1$; solid line), (2) strong water column denitrification feedback ($\alpha = 9$, $\beta = 1$, $\gamma = 1$; dotted line), and (3) both denitrification feedbacks strong ($\alpha = 9$, $\beta = 9$, $\gamma = 1$; dashed line).

both denitrification sensitivities are comparably strong ($\alpha = 9$, $\beta = 9$, $\gamma = 1$), the N fluxes and inventories lie between these two extreme cases.

[58] The evolution of nitrate $\delta^{15}N$ in these scenarios closely resembles the time history of the fraction of denitrification occurring in the water column. In the first scenario, this leads to a nearly monotonic increase in nitrate $\delta^{15}N$ in both the mean ocean and suboxic water columns. In the second case, both regions show large ^{15}N depletions into the Holocene, with interglacial nitrate $\delta^{15}N$ below the glacial values. While the suboxic zone shows a significant $\delta^{15}N$ maximum, the mean ocean does not. The f_w and nitrate $\delta^{15}N$ time series of the third case lie between these two extremes. The close correspondence between f_w and nitrate $\delta^{15}N$ in the scenarios with strong feedback shows that the isotopic history primarily reflects changes in the water column fraction of denitrification. This is because, in all three of these scenarios, glacial/interglacial changes in the nitrate inventory and in total denitrification rate are relatively minor.

3.2.3. Deglacial Experiments With Unequal Forcings

[59] We now investigate the impact of reduced climate forcing of sedimentary denitrification ($\phi = 0.3$, $\lambda = 0.6$). Experiments with equal denitrification forcings have pointed to the need for denitrification changes that restore f_w close to its glacial value in order to fit the observation that the $\delta^{15}N$ of mean ocean nitrate is similar during the Last Glacial Maximum and the later Holocene. Satisfying this condition when sediment denitrification forcing is weaker than the water column forcing requires that the strength of the sediment denitrification feedback also be weaker than the water column denitrification feedback. Figure 12 includes three such scenarios, one without a sediment denitrification feedback and weak overall feedback ($\alpha = 1$, $\beta = 0$, $\gamma = 1$), and

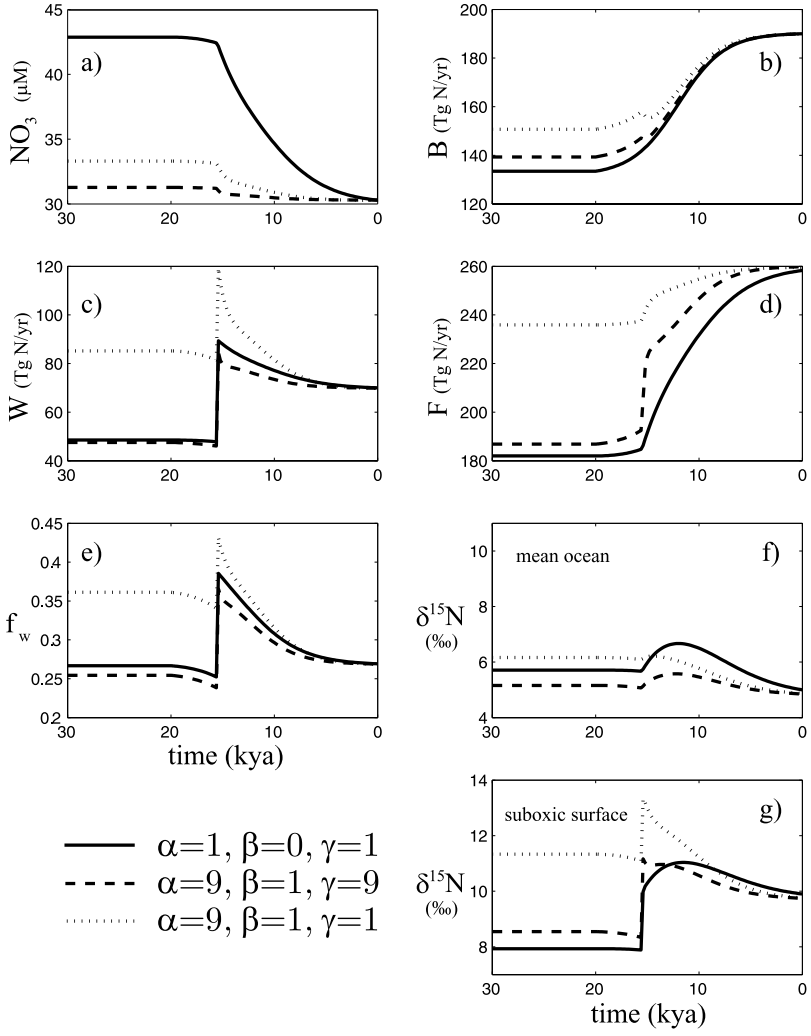

Figure 12. Same as Figure 9, but for three scenarios with reduced forcing of sediment denitrification ($\lambda = 0.6$, $\varphi = 0.3$): (1) no sedimentary denitrification feedback and weak overall feedback strength ($\alpha = 1$, $\beta = 0$, $\gamma = 1$; solid line), (2) strong feedbacks except for sedimentary denitrification, which is weak ($\alpha = 9$, $\beta = 1$, $\gamma = 9$; dashed line), and (3) weak feedbacks except for water column denitrification, which is strong ($\alpha = 9$, $\beta = 1$, $\gamma = 1$; dotted line).

two with weak sediment denitrification feedback but strong overall feedback ($\alpha = 9, \beta = 1, \gamma = 1$, and $\alpha = 9, \beta = 1, \gamma = 9$).

[60] In the case with weak overall feedback, a relatively strong water column denitrification feedback compensates for the strong climate forcing of water column denitrification, bringing f_w back to its glacial value. This is reflected in the evolution of nitrate $\delta^{15}N$ in the suboxic surface, which undergoes a deglacial maximum that resembles observed trends. However, this scenario allows a large (~40%) nitrate loss, and a large increase in the dilution effect therefore causes the nitrate $\delta^{15}N$ of the mean ocean to decrease by ~1‰ between glacial and interglacial steady states. This scenario is analogous to the previous scenario with denitrification forcings of equal magnitude in which all feedbacks are weakly operative (Figure 9, black curves).

[61] When all feedbacks are strengthened (from $\alpha = 1, \beta = 0, \gamma = 1$ to $\alpha = 9, \beta = 1, \gamma = 9$), the dilution effect is reduced while retaining a similar evolution of f_w. In this case, nitrate $\delta^{15}N$ in both the mean ocean and the suboxic surface reproduce the basic character of observed $\delta^{15}N$ trends. The relative sensitivities of water column and sediment denitrification feedbacks required to return f_w to its glacial value depend not only the strength of the climate forcings, but also on the strength of the N_2 fixation feedback. A N_2 fixation feedback that is much weaker than water column denitrification feedback ($\alpha = 9, \beta = 1, \gamma = 1$), causes a water column denitrification decrease that is too large, yielding a large decrease in f_w and therefore too low of a nitrate $\delta^{15}N$ in the later Holocene (Figure 12, dotted curves). If this combination of forcings is appropriate for the deglaciation, then a significant feedback from N_2 fixation is required. In the case of equal deglacial forcing of water column and sedimentary denitrification (sections 3.2.1 and 3.2.2), the N_2 fixation feedback was not crucial in matching observations. Thus the strength of the required N_2 fixation feedback depends on the assumptions that are made about the relative strength of

the deglacial forcings on water column and sedimentary denitrification.

3.2.4. Categorizing Responses in Terms of Forcing and Feedback Strength

[62] The salient features of the observed $\delta^{15}N$ records from sediment cores underlying the major suboxic zones of the modern ocean can be characterized by their deglacial $\delta^{15}N$ rise and Holocene $\delta^{15}N$ decrease. We estimate these parameters for a variety of published sediment cores, by subtracting average glacial and interglacial $\delta^{15}N$ values from the deglacial maximum. These parameters are plotted against each other in Figures 13a and Figures 13c, together with values from all model simulations. In most of the sediment cores, roughly half of the deglacial $\delta^{15}N$ rise is compensated by Holocene decreases. One core from the Gulf of California [*Pride et al.*, 1999] shows an exceptionally large Holocene $\delta^{15}N$ decrease (Figure 1).

[63] Among model simulations with equal forcings for water column and sedimentary denitrification and with strong overall feedback (Figure 13a), we can group the results into three categories. In the first group (top left) are those scenarios in which the sensitivity of water column denitrification feedback is much greater than that for sediment denitrification ($\alpha \ll \beta$). In these cases, sea level rise results in a large increase in sediment denitrification, while the strong feedback on denitrification in the water column restores that flux toward glacial values following the initial deglacial rise. The combination of these effects causes a large Holocene decrease in f_w, with a consequent net glacial-to-interglacial decrease in the nitrate $\delta^{15}N$ of both the global ocean and suboxic water column. A second cluster of scenarios shares the opposite relative denitrification sensitivities ($\alpha \ll \beta$). In these cases, the strong sedimentary denitrification feedback counteracts sea level rise, while the weak feedback for water column denitrification does little to reduce that flux following the forced deglacial increase. This results in step-like increases in f_w, with similarly evolving nitrate $\delta^{15}N$ in both the mean ocean and suboxic water column.

[64] The final cluster of model results is most similar to the available data, with Holocene decreases in $\delta^{15}N$ roughly half the magnitude of the deglacial rise. Results of this type are found in scenarios in which the sensitivities of both denitrification feedbacks are of similar strength ($\alpha \sim \beta$). Because denitrification forcings are equal in these scenarios, their feedback sensitivities must also be equal in order to prevent changes in water column denitrification from being much larger or much smaller than changes in sediment denitrification. Similarly, when the deglacial forcing of sediment denitrification is less than the water column denitrification forcing, the sensitivity of its feedback must also be reduced in order to satisfy data constraints (Figure 13c). This set of experiments further requires a strong N_2 fixation feedback, which competes with water column denitrification feedback, preventing water column denitrification from decreasing too strongly following its deglacial rise.

[65] Also shown in Figures 13a and 13c are the scenarios with weak overall feedback. In each set of experiments, only one scenario with weak overall feedback is consistent with the data constraints for suboxic surface $\delta^{15}N$. However, each of these scenarios ($\alpha = \beta = \gamma = 1$ when denitrification forcings are equal, and $\alpha = 1$, $\beta = 0$, $\gamma = 1$ when sediment denitrification forcing is reduced) violates the data constraint of no significant glacial-to-interglacial change in the $\delta^{15}N$ of nitrate in the mean ocean, due to the dilution effect (Figures 13b and 13d). It is therefore not possible to produce realistic isotope signals in an ocean with weak feedbacks. This means that isotope constraints on N cycle variations across the glacial/interglacial transition require an N budget that is tightly regulated by feedbacks either through N_2 fixation, denitrification or both. None of the scenarios we examined with a N inventory change exceeding 30% was able to produce isotope trends consistent with the observations in both the mean ocean and the suboxic surface. We believe it is unlikely that any scenarios with N inventory changes greater than 20% will be able to satisfy these constraints. Among the scenarios that best matched the sedimentary data, the maximum magnitude of N inventory changes is less than 10%.

[66] There are several independent indications in the geologic record for the existence of a water column denitrification feedback. First, a number of sediment cores from the open eastern North Pacific margin indicate a return to bioturbation following a laminated deglacial interval. *Ganeshram and Pedersen* [1998] and *Pride et al.* [1999] have observed that cores from the Mexican margin at depths of 800–1000 m contain bioturbated sediments beginning

Figure 13. Deglacial $\delta^{15}N$ increase (maximum minus glacial) versus Holocene $\delta^{15}N$ decrease (maximum minus modern) in (a, c) the surface of the suboxic water column and (b, d) the mean ocean from model simulations (open circles) with equal denitrification forcings ($\lambda = \varphi = 0.6$; Figures 13a and 13b) and with reduced sediment denitrification forcing ($\lambda = 0.6$ $\varphi = 0.3$; Figures 13c and 13d). Stars represent values estimated from published sediment cores: 893A [*Emmer and Thunell*, 2000]; NH15P, 1017E, NH22P [Ganeshram et al., 2000]; JPC56 [*Pride et al.*, 1999]; Arabian Sea [*Suthhof et al.*, 2001], and Mexican Margin [*Thunell and Kepple*, 2004]. Lines indicate fraction of deglacial $\delta^{15}N$ increase that is subsequently compensated by a deglacial-to-Holocene decrease: 100% (solid line) or 50% and 25% (dashed lines). Model points are identified according to their sensitivity values with the order $\alpha\beta\gamma$ (e.g., 910 refers to the experiment with $\alpha = 9$, $\beta = 1$, $\gamma = 0$). Clusters of experiments with strong overall feedbacks are grouped by ovals: (1) water column denitrification sensitivity much larger than sediment denitrification sensitivity ($\alpha \gg \beta$, black oval), (2) sediment denitrification sensitivity much larger than water column denitrification sensitivity ($\beta \gg \alpha$, light gray oval), and (3) both denitrification sensitivities on par, i.e., either both weak/off or both strong ($\alpha \sim \beta$, medium gray oval). For each cluster, a representative trajectory of $\delta^{15}N$ in the suboxic surface is shown (insets, Figure 13a) using corresponding gray shade. Experiments with weak overall sensitivity are also shown. The sloping gray oval (Figure 13b) indicates mean ocean changes that appear most likely given current sediment $\delta^{15}N$ records representative of the mean ocean [*Holmes et al.*, 1997; *Kienast*, 2000; N. Meckler, unpublished data].

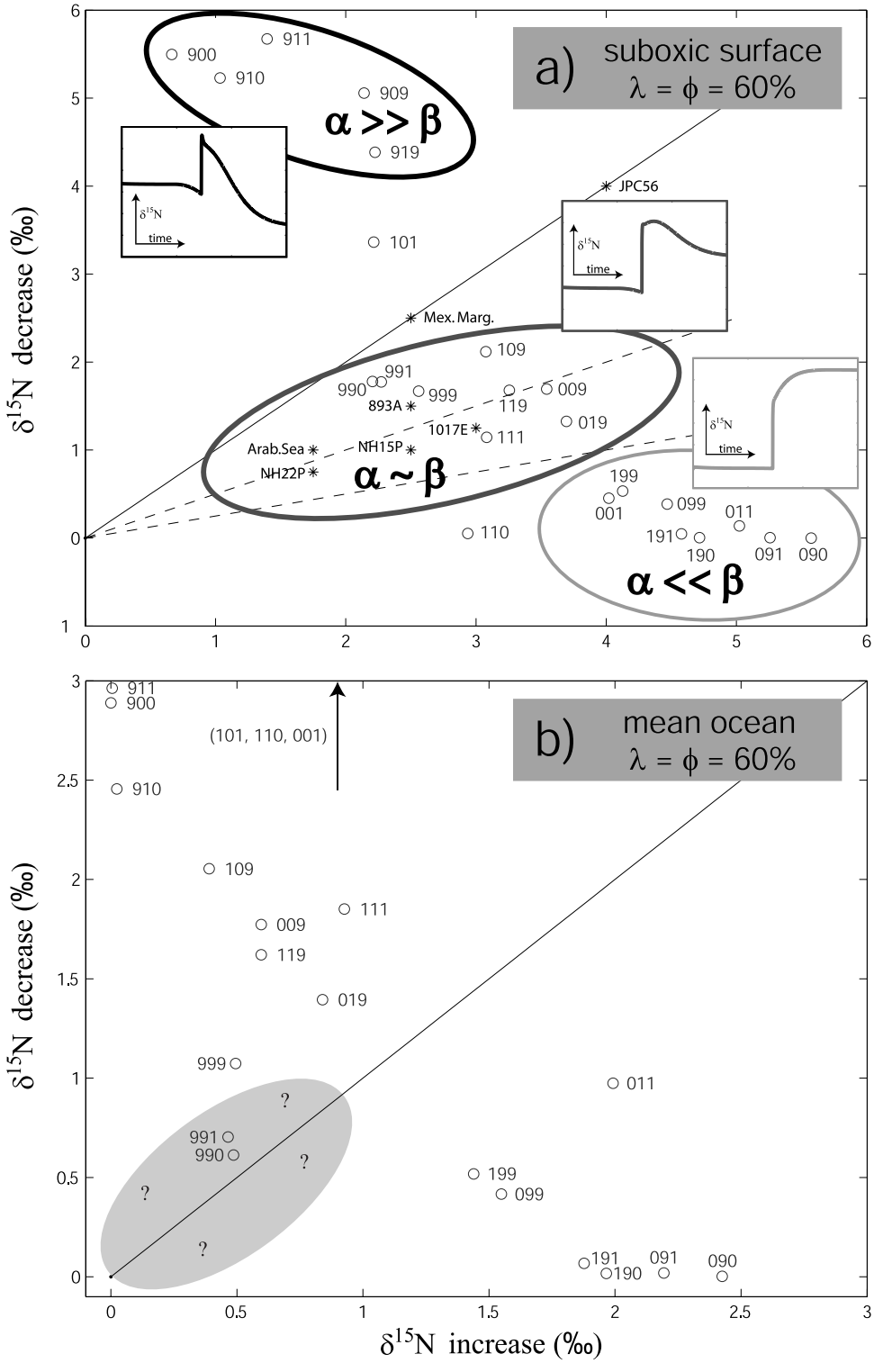
a)
suboxic surface
λ = ϕ = 60%
α >> β
α ~ β
α << β
JPC56
Mex. Marg.
Arab.Sea
NH15P
NH22P
893A
1017E
δ15N decrease (‰)
b)
mean ocean
λ = ϕ = 60%
(101, 110, 001)
δ15N increase (‰)

Figure 13

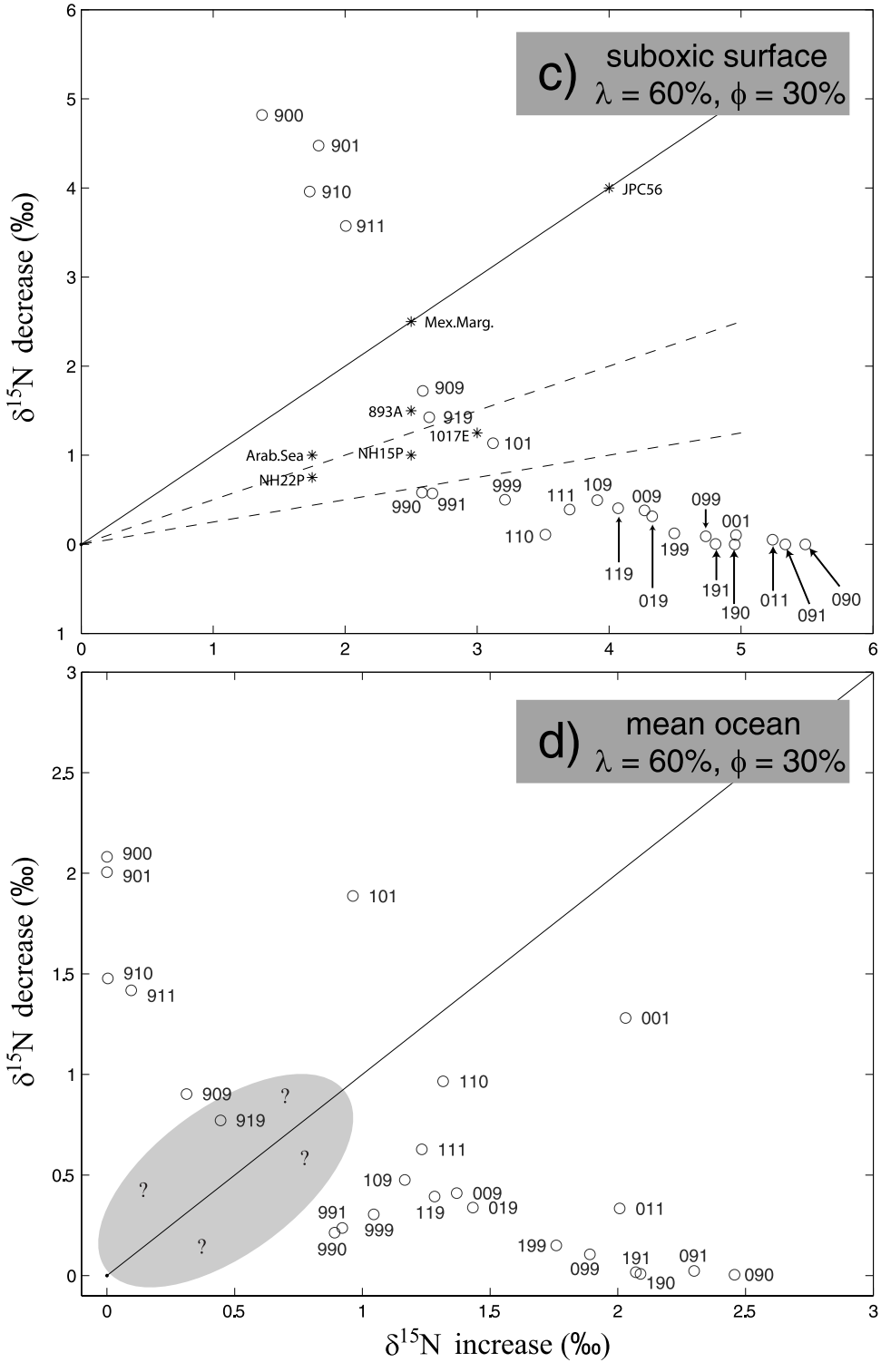

Figure 13. (continued)

between 6 and 8 kya. Several locations along the California margin also reveal laminated deglacial intervals giving way to bioturbation, though the laminated portion of these cores is much shorter [*Zheng et al.*, 2000]. In addition, Mo deposition indicative of highly reducing conditions is observed in these locations during the Bolling-Allerod, indicating a contraction of the early deglacial oxygen minimum zone (OMZ) subsequent to that time period, toward today's suboxic zone centered on the Mexican margin [*Zheng et al.*, 2000].

[67] These cores are all found near the base of the modern OMZ, suggesting that the bottom of the OMZ has shoaled

in the Holocene. Further evidence for a shoaling of the base of the OMZ comes from *Cannariato and Kennett* [1999], who conclude, on the basis of foraminiferal assemblages, that the depth of the suboxic layer in the Gulf of California contracted following a deglacial expansion. The combination of these records supports a scenario in which the suboxic zone receded following its deglacial apex, horizontally and/or vertically. While a causal role for ventilation changes cannot be ruled out, these observations would indeed be expected from the denitrification feedback described above. That is, increased denitrification at the end of the last ice age would have reduced the nitrate inventory, globally and locally, leading to lower export production and thus higher subsurface [O_2].

[68] Finally, it is likely to be difficult to reconstruct glacial/interglacial forcing of denitrification fluxes, especially for the sediments. However, for a given deglacial forcing of water column and sedimentary denitrification, the transient behavior of N isotopes provides a constraint on the relative sensitivity of denitrification feedbacks. If denitrification forcing in the water column and sediments are of equal magnitude, their feedback sensitivities must also be similar, whereas a stronger climate-forced increase in water column denitrification requires that this flux also have a stronger feedback. That is, a mechanistic understanding of the N budget feedbacks parameterized here would make it possible to reconstruct the deglacial forcing on denitrification fluxes.

4. Conclusions

[69] As more high-resolution sediment records of sediment $\delta^{15}N$ have become available, new features can be seen across a wide variety of oceanic regions. One of these is a late deglacial/early Holocene decrease in the $\delta^{15}N$ of surface nitrate in the suboxic water column. This decrease, which follows the well-known deglacial $\delta^{15}N$ rise in these regions [*Altabet et al.*, 1995; *Ganeshram et al.*, 1995], results in a transient deglacial maximum of suboxic nitrate $\delta^{15}N$. While the mean $\delta^{15}N$ of nitrate appears to be similar in the glacial and interglacial ocean [*Kienast*, 2000], recent sedimentary records suggest that the whole ocean may exhibit a peak in $\delta^{15}N$ upon deglaciation, but with smaller amplitude [*Holmes et al.*, 1997; *Kienast*, 2000].

[70] Because the fraction of total denitrification occurring in the water column, f_w, is the dominant control on the steady state $\delta^{15}N$ of ocean nitrate [*Brandes and Devol*, 2002], producing a deglacial $\delta^{15}N$ maximum requires deglacial N budget changes that involve a transient maximum in f_w. An initial increase in f_w can be explained by a climate-forced increase in water column denitrification upon deglaciation [*Altabet et al.*, 1995; *Ganeshram et al.*, 1995]. A subsequent f_w decrease could occur through a lagged increase in sediment denitrification due to sea level rise, and may be strengthened through a negative feedback between denitrification and the declining ocean N inventory, if that feedback is stronger in the water column than in the sediments. The similarity of mean ocean nitrate $\delta^{15}N$ in glacial and interglacial periods implies that the net effect of deglacial climate forcing and internal feedbacks tends to restore the glacial partitioning of denitrification between the water column and sediments. The decrease in f_w during the late deglacial/Holocene was therefore comparable to its early deglacial increase.

[71] The size of the nitrate inventory and the total denitrification rate are secondary but significant factors determining the steady state ocean nitrate $\delta^{15}N$. As the nitrate inventory decreases and/or the total denitrification rate increases (with constant f_w), the degree of nitrate consumption in the suboxic zone increases. This elevated consumption of suboxic zone nitrate causes its $\delta^{15}N$ to increase due to isotopic fractionation, but causes mean ocean nitrate $\delta^{15}N$ to decrease, due to the reduced influence of the residual suboxic nitrate on the rest of the ocean. Glacial/interglacial changes in the ocean nitrate inventory and the total denitrification rate therefore cause the evolution of nitrate $\delta^{15}N$ in the mean ocean and the suboxic zone to deviate in opposite directions from the trends that would be expected on the basis of f_w alone. When nitrate losses are large, a significant suboxic $\delta^{15}N$ maximum during deglaciation can only occur with a very pronounced maximum in f_w; that is, when late deglacial/Holocene f_w decrease is as large or larger than the early deglacial increase. However, a large f_w decrease, combined with a large nitrate loss, results in a large glacial-to-interglacial decline in mean ocean $\delta^{15}N$ due to the dilution effect, which is not supported by current sedimentary records. For this reason, it is not possible to simultaneously satisfy data constraints from the mean ocean and the suboxic water column when N losses are large.

[72] Satisfying data constraints from both the suboxic zone and the mean ocean therefore requires (1) that f_w return toward its glacial value and (2) that glacial-to-interglacial total nitrate losses are relatively small. These two requirements, in turn, place constraints on the strength of the various feedbacks. First, limiting the oceanic loss of nitrate requires strong feedbacks by either N_2 fixation or denitrification. Whether we can distinguish between strong N_2 fixation feedback and strong denitrification feedback as the source of N budget regulation on the basis of N isotopic constraints depends on the deglacial forcing on denitrification, which is not well known. However, there are other geologic indications that a water column denitrification feedback may have been operative since the Last Glacial Maximum.

[73] Second, the relative sensitivities of water column and sediment denitrification feedbacks must be proportional to their relative climate forcing. If both denitrification forcings are of similar magnitude, their feedbacks must also be of similar strength in order to reduce f_w back toward, but not beyond, its glacial level. Thus, if deglacial forcing of water column denitrification was stronger than the forcing of sediment denitrification, its feedback must also be stronger. Since sediment denitrification is controlled primarily by the flux of organic carbon to the sediments, rather than by the oxygenation of the overlying water, a relatively weak feedback for sedimentary denitrification seems sensible. This suggests, in turn, that the deglacial forcing on water column denitrification was proportionally greater than that on sedimentary denitrification.

[74] Finally, these results have important implications for theories of glacial/interglacial atmospheric CO_2 changes that rely on changes in oceanic nutrient inventory. Our results

suggest that in order to reproduce isotope trends across the last deglacial transition, N inventory changes should not have been larger than 30%, and they are likely to have been much smaller. The impact on atmospheric CO_2 of a change in nutrient reservoir of this magnitude depends significantly on the model used. In box models [e.g., *Sarmiento and Toggweiler*, 1984], atmospheric CO_2 is less sensitive to low-latitude productivity changes than high latitudes, whereas general circulation models are more sensitive to low-latitude perturbations [*Broecker et al.*, 1999].

[75] Using a box model with an intermediate sensitivity, *Sigman et al.* [1998] find that increased low-latitude productivity resulting from an increase in nutrient reservoir of 30% produces a pCO_2 reduction of 34 ppm if $CaCO_3$ effects are neglected. If transient and equilibrium constraints on the calcite lysocline are included, the pCO_2 change is 17–45 ppm, depending on assumptions about $CaCO_3$ production [*Sigman et al.*, 1998]. Thus it appears that glacial N reservoir increases allowed by the constraints imposed by the sedimentary $\delta^{15}N$ cannot account for the dominant part of the observed 80–90 ppm glacial decrease in atmospheric CO_2.

[76] **Acknowledgments.** C. D. was supported by NASA Headquarters under an Earth System Science Fellowship grant NGT5-30356. D. M. S. was supported by NSF grants OCE-9981479, OCE-0136449, and DEB-0083566 (to Simon Levin), and by British Petroleum and Ford Motor Company through the Princeton Carbon Mitigation Initiative. We thank Jorge Sarmiento for improving the manuscript through his careful reading and thoughtful comments.

References

Altabet, M. A. (1988), Variations in nitrogen isotopic composition between sinking and suspended particles: Implications for nitrogen cycling and particle transformation in the open ocean, *Deep Sea Res., Part I*, *35*, 535–554.

Altabet, M. A., R. Francois, D. W. Murray, and W. L. Prell (1995), Climate-related variations in denitrification in the Arabian Sea from sediment $^{15}N/^{14}N$ ratios, *Nature*, *373*, 506–509.

Altabet, M. A., C. Pilskaln, R. Thunell, C. Pride, D. Sigman, F. Chavez, and R. Francois (1999), The nitrogen isotope biogeochemistry of sinking particles from the margin of the eastern North Pacific, *Deep Sea Res., Part I*, *46*, 655–679.

Altabet, M. A., M. J. Higginson, and D. W. Murray (2002), The effect of millennial-scale changes in Arabian Sea denitrification on atmospheric CO_2, *Nature*, *415*, 159–162.

Bard, E., B. Hamelin, R. G. Fairbanks, and A. Zindler (1990), Calibration of the C-14 timescale over the past 30,000 years using mass-spectrometric U-Th ages from Barbados corals, *Nature*, *345*, 405–410.

Barford, C. C., J. P. Montoya, M. A. Altabet, and R. Mitchell (1999), Steady-state nitrogen isotope effects of N_2 and N_2O production in *Paracoccus denitrificans*, *Appl. Environ. Microbiol.*, *65*, 989–994.

Blunier, T., B. Barnett, M. L. Bender, and M. B. Hendricks (2002), Biological oxygen productivity during the last 60,000 years from triple oxygen isotope measurements, *Global Biogeochem. Cycles*, *16*(3), 1029, doi:10.1029/2001GB001460.

Brandes, J. A., and A. H. Devol (1997), Isotopic fractionation of oxygen and nitrogen in coastal marine sediments, *Geochim. Cosmochim. Acta*, *61*, 1793–1801.

Brandes, J. A., and A. H. Devol (2002), A global marine fixed nitrogen isotopic budget: Implications for Holocene nitrogen cycling, *Global Biogeochem. Cycles*, *16*(4), 1120, doi:10.1029/2001GB001856.

Brandes, J. A., A. H. Devol, T. Yoshinari, D. A. Jayakumar, and S. W. A. Naqvi (1998), Isotopic composition of nitrate in the central Arabian Sea and eastern tropical North Pacific: A tracer for mixing and nitrogen cycles, *Limnol. Oceanogr.*, *43*, 1680–1689.

Broecker, W. S. (1982a), Glacial to interglacial changes in ocean chemistry, *Prog. Oceanogr.*, *2*, 151–197.

Broecker, W. S. (1982b), Ocean chemistry during glacial time, *Geochim. Cosmochim. Acta*, *46*, 1689–1706.

Broecker, W. S., and G. M. Henderson (1998), The sequence of events surrounding Termination II and their implications for the cause of glacial-interglacial CO_2 changes, *Paleoceanography*, *13*, 352–364.

Broecker, W. S., and T.-H. Peng (1987), The role of $CaCO_3$ compensation in the glacial to interglacial atmospheric CO_2 change, *Global Biogeochem. Cycles*, *1*, 15–29.

Broecker, W. S., J. Lynch-Stieglitz, D. Archer, M. Hofmann, E. Maier-Reimer, O. Marchal, T. Stocker, and N. Gruber (1999), How strong is the Harvardton-Bear constraint?, *Global Biogeochem. Cycles*, *13*, 817–820.

Cannariato, K. G., and J. P. Kennett (1999), Climatically related millennial-scale fluctuations in strength of California margin oxygen-minimum zone during the past 60 k.y., *Geology*, *27*, 975–978.

Carpenter, E., H. Harvey, B. Fry, and D. Capone (1997), Biogeochemical tracers of the marine cyanobacterium Trichodesmium, *Deep Sea Res., Part I*, *44*, 27–38.

Christensen, J. P. (1994), Carbon export from continental shelves, denitrification and atmospheric carbon dioxide, *Cont. Shelf Res.*, *14*, 547–576.

Christensen, J. P., J. W. Murray, A. H. Devol, and L. A. Codispoti (1987), Denitrification in continental shelf sediments has major impact on the oceanic nitrogen budget, *Global Biogeochem. Cycles*, *1*, 97–116.

Codispoti, L. A. (1989), Phosphorus vs. nitrogen limitation of new and export production, in *Productivity of the Ocean: Past and Present*, edited by W. H. Berger, V. S. Smetacek, and G. Wefer, pp. 377–394, John Wiley, Hoboken, N. J.

Codispoti, L. A., and J. P. Christensen (1985), Nitrification, denitrification, and nitrous oxide cycling in the eastern tropical Pacific Ocean, *Mar. Chem.*, *16*, 277–300.

Conkright, M., S. Levitus, and T. Boyer (1994), *World Ocean Atlas 1994*, vol. 1. *Nutrients*, *NOAA Atlas NESDIS 1*, 16 pp., Natl. Oceanic and Atmos. Admin., Silver Spring, Md.

Deutsch, C., N. Gruber, R. M. Key, J. L. Sarmiento, and A. Ganaschaud (2001), Denitrification and N_2 fixation in the Pacific Ocean, *Global Biogeochem. Cycles*, *15*, 483–506.

Devol, A. H. (1991), Direct measurement of nitrogen gas fluxes from continental shelf sediments, *Nature*, *349*, 319–321.

Emmer, E., and R. C. Thunell (2000), Nitrogen isotope variations in Santa Barbara Basin sediments: Implications for denitrification in the eastern tropical North Pacific during the last 50,000 years, *Paleoceanography*, *15*, 377–387.

Falkowski, P. G. (1997), Evolution of the nitrogen cycle and its influence on the biological sequestration of CO_2 in the ocean, *Nature*, *387*, 272–275.

Francois, R. F., M. A. Altabet, E.-F. Yu, D. M. Sigman, M. P. Bacon, M. Frank, G. Bohrmann, G. Bareille, and L. D. Labeyrie (1997), Water column stratification in the Southern Ocean contributed to the lowering of glacial atmospheric CO_2, *Nature*, *389*, 929–935.

Ganeshram, R. S., and T. F. Pedersen (1998), Glacial-interglacial variability in upwelling and bioproductivity off northwest Mexico: Implications for quaternary paleoclimate, *Paleoceanography*, *13*, 634–645.

Ganeshram, R. S., T. F. Pedersen, S. E. Calvert, and J. W. Murray (1995), Large changes in oceanic nutrient inventories from glacial to interglacial periods, *Nature*, *376*, 755–758.

Ganeshram, R. S., T. F. Pedersen, S. E. Calvert, G. W. McNeill, and M. R. Fontugne (2000), Glacial-interglacial variability in denitrification in the world's oceans: Causes and consequences, *Paleoceanography*, *15*, 361–376.

Ganeshram, R. S., T. F. Pedersen, S. E. Calvert, and R. Francois (2002), Reduced nitrogen fixation in the glacial ocean inferred from changes in marine nitrogen and phosphorus inventories, *Nature*, *415*, 156–159.

Gruber, N., and J. L. Sarmiento (1997), Global patterns of marine nitrogen fixation and denitrification, *Global Biogeochem. Cycles*, *11*, 235–266.

Hanebuth, T., K. Stattegger, and P. M. Grootes (2000), Rapid flooding of the Sunda Shelf: A late-glacial sea-level record, *Science*, *288*, 1033–1035.

Haug, G. H., T. F. Pedersen, D. M. Sigman, S. E. Calvert, B. Nielsen, and L. C. Peterson (1998), Glacial/interglacial variations in productivity and nitrogen fixation in the Cariaco Basin during the last 550 ka, *Paleoceanography*, *13*, 427–432.

Holmes, M. E., R. R. Schneider, P. J. Müller, M. Segl, and G. Wefer (1997), Reconstruction of past nutrient utilization in the eastern Angola Basin based on sedimentary $^{15}N/^{14}N$ ratios, *Paleoceanography*, *12*, 604–614.

Karl, D., R. Letelier, L. Tupas, J. Dore, J. Christian, and D. Hebel (1997), The role of nitrogen fixation in biogeochemical cycling in the subtropical North Pacific Ocean, *Nature*, *388*, 533–538.

Karl, D., A. Michaels, B. Bergman, D. Capone, E. Carpenter, R. Letelier, F. Lipschultz, H. Paerl, D. Sigman, and L. Stal (2002), Dinitrogen fixation in the world's oceans, *Biogeochemistry*, *57/58*, 47–98.

Keigwin, L. D., and G. A. Jones (1990), Deglacial climatic oscillations in the Gulf of California, *Paleoceanography*, *5*, 1009–1023.

Kennett, J. P., and B. L. Ingram (1995), A 20,000-year record of ocean circulation and climate change from the Santa Barbara basin, *Nature*, *377*, 510–514.

Kienast, M. (2000), Unchanged nitrogen isotopic composition of organic matter in the South China Sea during the last climatic cycle: Global implications, *Paleoceanography*, *15*, 244–253.

Liu, K.-K., and I. R. Kaplan (1989), The eastern tropical Pacific as a source of ^{15}N-enriched nitrate in seawater off southern California, *Limnol. Oceanogr.*, *34*, 820–830.

Martin, J. H., G. A. Knauer, D. M. Karl, and W. W. Broenkow (1987), VERTEX: Carbon cycling in the northeast Pacific, *Deep Sea Res.*, *34*, 267–285.

Matsumoto, K., J. L. Sarmiento, and M. A. Brzezinski (2002), Silicic acid leakage from the Southern Ocean as a possible mechanism for explaining glacial atmospheric pCO_2, *Global Biogeochem. Cycles*, *16*(3), 1031, doi:10.1029/2001GB001442.

McElroy, M. B. (1983), Marine biological controls on atmospheric CO_2 and climate, *Nature*, *302*, 328–329.

Middelburg, J. J., K. Soetaert, P. M. J. Herman, and C. H. R. Heip (1996), Denitrification in marine sediments: A model study, *Global Biogeochem. Cycles*, *10*, 661–673.

Pride, C., R. Thunell, D. Sigman, L. Keigwin, M. Altabet, and E. Tappa (1999), Nitrogen isotopic variations in the Gulf of California since the last deglaciation: Response to global climate change, *Paleoceanography*, *14*, 397–409.

Redfield, A. C., B. H. Ketchum, and F. A. Richards (1963), The influence of organisms on the composition of seawater, in *The Sea*, vol. 2, edited by M. N. Hill, pp. 26–77, Wiley-Intersci., Hoboken, N. J.

Sarmiento, J. L., and J. R. Toggweiler (1984), A new model for the role of the oceans in determining atmospheric pCO_2, *Nature*, *308*, 621–624.

Sigman, D. M., and K. L. Casciotti (2001), Nitrogen isotopes in the ocean, in *Encyclopedia of Ocean Sciences*, edited by J. H. Steele, K. K. Turekian, and S. A. Thorpe, pp. 1884–1894, Academic, San Diego, Calif.

Sigman, D. M., and G. H. Haug (2003), Biological pump in the past, in *Treatise On Geochemistry*, edited by H. D. Holland, K. K. Turekian, and H. Elderfield, pp. 491–528, Elsevier Sci., New York.

Sigman, D. M., D. C. McCorkle, and W. R. Martin (1998), The calcite lysocline as a constraint on glacial/interglacial low-latitude production changes, *Global Biogeochem. Cycles*, *12*, 409–427.

Sigman, D. M., M. A. Altabet, R. Francois, D. C. McCorkle, and G. Fischer (1999), The $\delta^{15}N$ of nitrate in the Southern Ocean: Consumption of nitrate in surface waters, *Global Biogeochem. Cycles*, *13*, 1149–1166.

Sigman, D. M., M. A. Altabet, D. C. McCorkle, R. Francois, and G. Fischer (2000), The $\delta^{15}N$ of nitrate in the Southern Ocean: Nitrogen cycling and circulation in the ocean interior, *J. Geophys. Res.*, *105*, 19,599–19,614.

Sigman, D. M., R. Robinson, A. N. Knapp, A. van Geen, D. C. McCorkle, J. A. Brandes, and R. C. Thunell (2003), Distinguishing between water column and sedimentary denitrification in the Santa Barbara Basin using the stable isotopes of nitrate, *Geochem. Geophys. Geosyst.*, *4*, 1040, doi:10.1029/2002GC000384.

Suthhof, A., V. Ittekkot, and B. Gaye-Haake (2001), Millennial-scale oscillation of denitrification intensity in the Arabian Sea during the late Quaternary and its potential influence on atmospheric N_2O and global climate, *Global Biogeochem. Cycles*, *15*, 637–649.

Thunell, R. C., and A. Kepple (2004), Glacial-Holocene $\delta^{15}N$ record from the Gulf of Tehuantepec, Mexico: Implications for denitrification in the eastern equatorial Pacific and changes in atmospheric N_2O, *Global Biogeochem. Cycles*, *18*, GB1001, doi:10.1029/2002GB002028.

Thunell, R. C., D. M. Sigman, F. Muller-Karger, Y. Astor, and R. Varela (2004), Nitrogen isotope dynamics of the Cariaco Basin, Venezuela, *Global Biogeochem. Cycles*, *18*, GB3001, doi:10.1029/2003GB002185.

Toggweiler, J. R., and S. Carson (1995), What are the upwelling systems contributing to the ocean's carbon and nutrient budgets?, in *Upwelling in the Ocean: Modern Processes and Ancient Records*, edited by C. P. Summerhayes et al., John Wiley, Hoboken, N. J.

Tyrrell, T. (1999), The relative influences of nitrogen and phosphorus on oceanic primary production, *Nature*, *400*, 525–531.

Van Mooy, B. A. S., R. G. Keil, and A. H. Devol (2002), Impact of suboxia on sinking particulate organic carbon: Enhanced carbon flux and preferential degradation of amino acids via denitrification, *Geochim. Cosmochim. Acta*, *66*, 457–465.

Voss, M., J. W. Dippner, and J. P. Montoya (2001), Nitrogen isotope patterns in the oxygen-deficient waters of the eastern tropical North Pacific Ocean, *Deep Sea Res., Part I*, *48*, 1905–1921.

Zheng, Y., R. F. Anderson, A. van Geen, and J. Kuwabara (2000), Authigenic molybdenum formation in marine sediments: A link to pore water sulfide in the Santa Barbara Basin, *Geochim. Cosmochim. Acta*, *64*, 4165–4178.

C. Deutsch, Program on Climate Change, University of Washington, 407 OSB, Box 357940, Seattle, WA 98195-7940, USA. (cdeutsch@ocean.washington.edu)

G. H. Haug, Geoforschungszentrum Potsdam, Telegrafenberg, D-14473 Potsdam, Germany. (haug@gfz-potsdam.de)

A. N. Meckler, Geological Institute, ETH Zentrum, Sonneggstrasse 5, Ch-8092 Zurich, Switzerland. (nele.meckler@erdw.ethz.ch)

D. M. Sigman, Department of Geosciences, Princeton University, Guyot Hall, Princeton, NJ 08544, USA. (sigman@princeton.edu)

R. C. Thunell, Department of Geological Sciences, University of South Carolina, Columbia, SC 29208, USA. (thunell@geol.sc.edu)

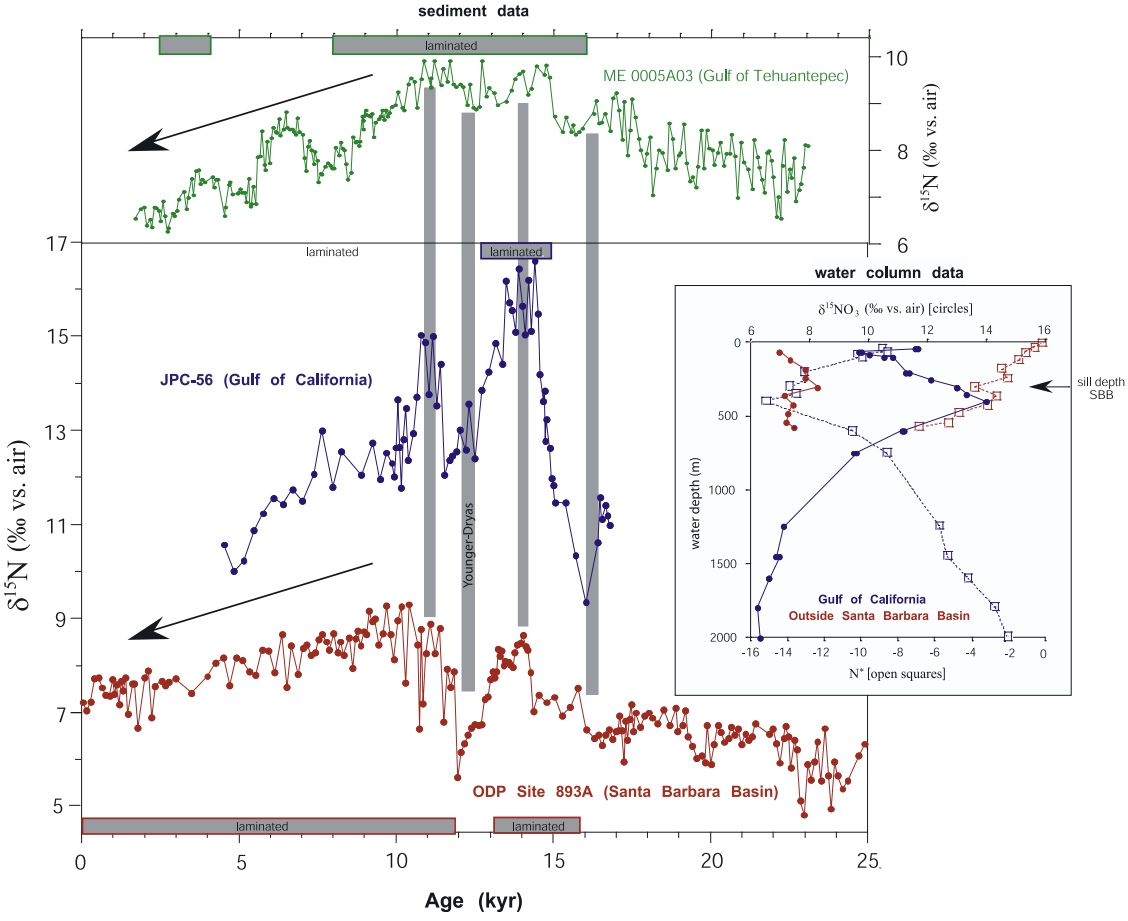

Figure 1. Downcore records of bulk sediment $\delta^{15}N$ from the eastern North Pacific (Gulf of Tehuantepec, Mexican margin [*Thunell and Kepple*, 2004]; Gulf of California [*Pride et al.*, 1999]; and Santa Barbara Basin [*Emmer and Thunell*, 2000]). Intervals of sediment lamination are indicated with a gray bar for each record. The Mexican margin and the Gulf of California are regions of active water column denitrification today, whereas the waters overlying the Santa Barbara Basin are influenced by the northward advection (in the California Undercurrent) of the denitrification signal from the south (nitrate $\delta^{15}N$ (solid circles) and N* (open squares) shown in inset [*Altabet et al.*, 1999; *Sigman et al.*, 2003]).

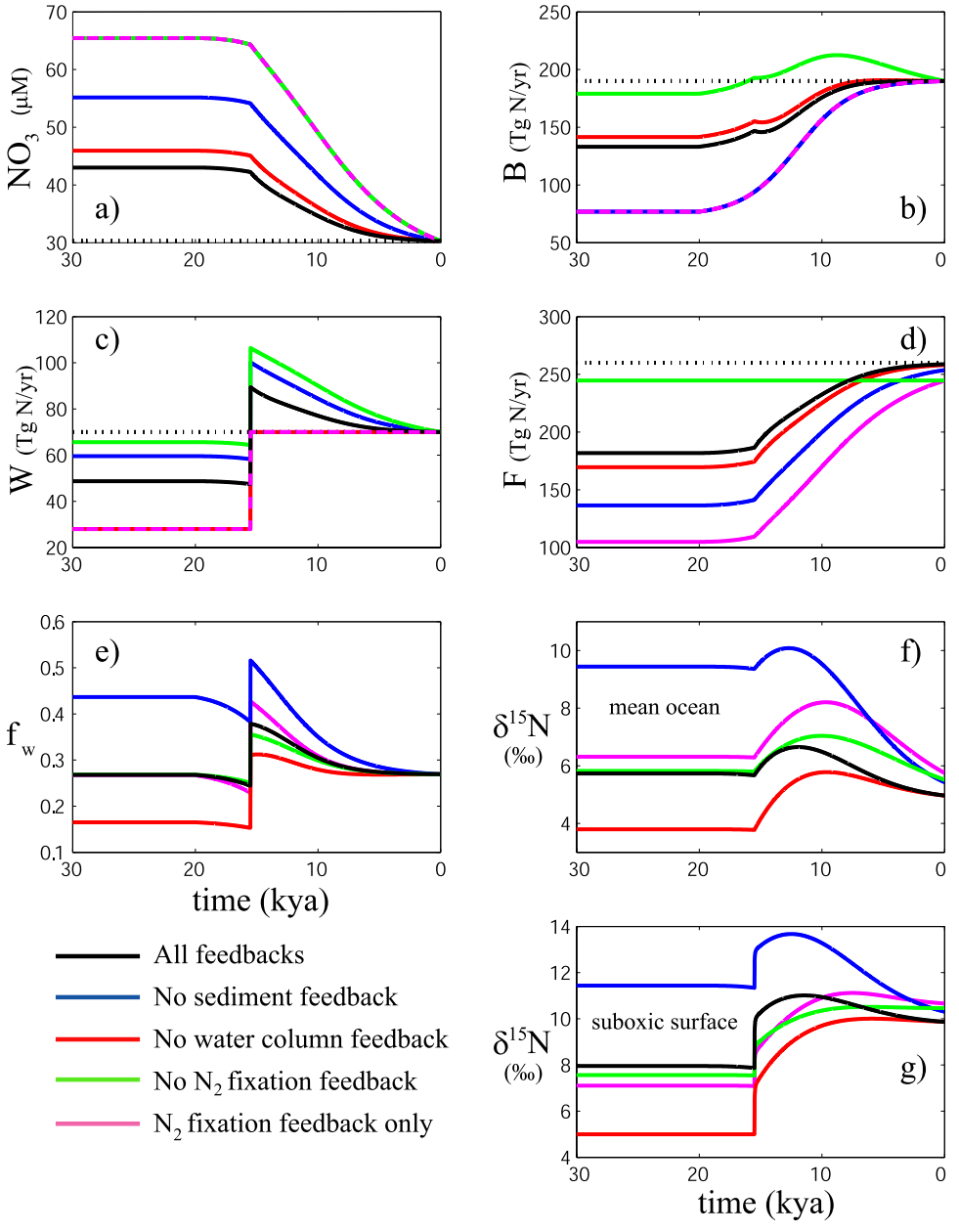

Figure 9. Time series of key variables in five scenarios with equal forcing of sediment and water column denitrification ($\lambda = \varphi = 0.6$) and weak overall N budget feedback. Variables are (a) mean ocean nitrate concentration ($[NO_3^-]$), (b) sedimentary denitrification (B), (c) water column denitrification (W), (d) N_2 fixation (F), (e) fraction of total denitrification occurring in the water column (f_w), (f) $\delta^{15}N$ for the surface box of the suboxic water column, and (g) mean ocean $\delta^{15}N$. Five model scenarios with weak overall feedbacks are shown: (1) all feedbacks on ($\alpha = \beta = \gamma = 1$; black dashed line (black in color version)), (2) no sedimentary denitrification feedback ($\alpha = 1$, $\beta = 0$, $\gamma = 1$; gray solid line (blue in color version)), (3) no water column denitrification feedback ($\alpha = 0$, $\beta = \gamma = 1$; gray dashed line (red in color version)), (4) no N_2 fixation feedback ($\alpha = \beta = 1$, $\gamma = 0$; gray dash-dotted line (green in color version)), and (5) N_2 fixation feedback only ($\alpha = \beta = 0$, $\gamma = 1$; black dotted line (pink in color version)). Each experiment is run for 30,000 years, starting from a glacial steady state that is determined by requiring N inventory and denitrification fluxes to reach modern values (thin black lines) at the end of the simulation.

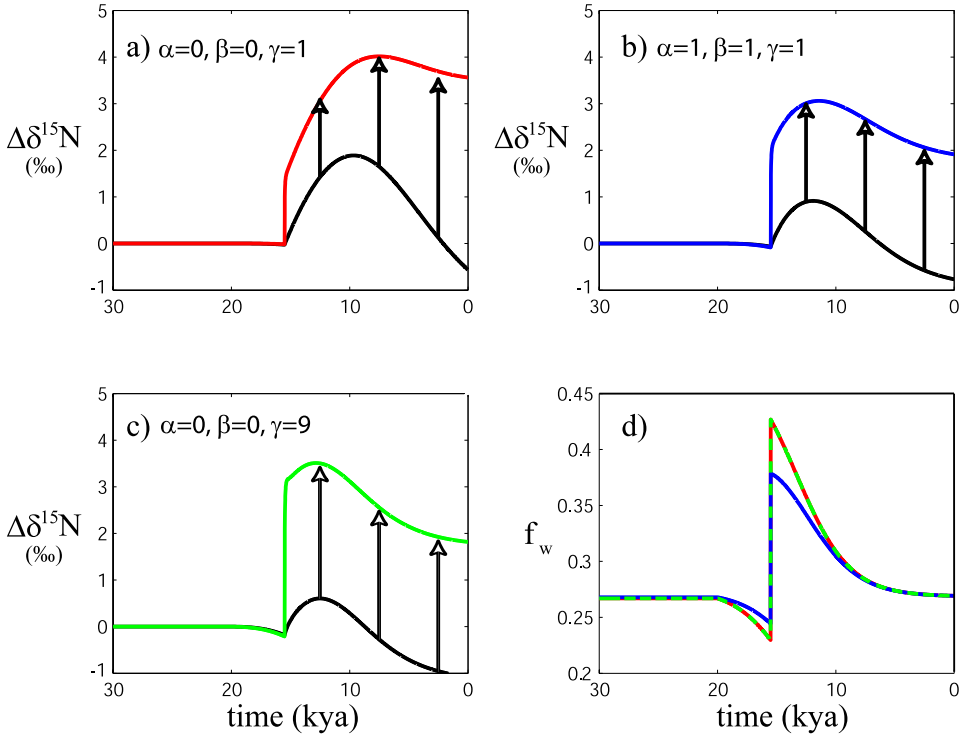

Figure 10. Changes in nitrate $\delta^{15}N$ in the mean ocean (dotted lines) and surface waters, overlying the suboxic zone for three scenarios, each with $\lambda = \varphi = 0.6$: (a) weak N_2 fixation feedback only ($\alpha = \beta = 0$; $\gamma = 1$, gray solid line (red in color version)), (b) all feedbacks operative but weak ($\alpha = \beta = 1$; $\gamma = 1$, black solid line (blue in color version)), and (c) strong N_2 fixation feedback only ($\alpha = \beta = 0$; $\gamma = 9$, black dashed line (green in color version)). (d) The fraction of denitrification occurring in the water column, f_w, is roughly the same in all cases. The differences in isotopic evolution of the mean ocean versus surface waters overlying the suboxic zone are due to nitrate consumption in the suboxic zone. Increased consumption of suboxic N throughout the Holocene leads to the divergence between mean ocean and suboxic $\delta^{15}N$ (Figure 10a), causing larger suboxic $\delta^{15}N$ increases and smaller subsequent decreases.